CONTINUOUSLY RENEWED COPPER ELECTRODE FOR AMPEROMETRIC MEASUREMENT OF CARBOHYDRATES

A Thesis

Presented to

The Faculty of the Department of Chemistry and Biochemistry

University of Texas at Arlington

In Partial Fulfillment

of the Requirements for the Degree of

Masters of Science in Chemistry

August, 2021

By

Shane Wilson

Arlington, Texas

Abstract. Currently the benchmark method for carbohydrate analysis in a variety of application areas involves anion exchange chromatography followed by electrochemical detection at a gold electrode. The gold electrode surfaces foul from deposition of oxidation products over time; pulsed waveforms with oxidative cleaning and surface reduction are used to improve electrode longevity. After fouling, the electrode needs polishing, or, if using disposable gold electrodes, replacement; both remedies require subsequent recalibration. I describe here a novel electrochemical amperometric detector using a copper electrode that is consumed during the measurement process and a new surface is continuously generated without a change in the electrode distance/placement geometry. A copper wire acts as the working electrode; a stainless-steel tube acts as the counter electrode and also the cell inlet. At the working potential, a thin layer of copper oxide exists at equilibrium on the electrode surface. As carbohydrates contact the working electrode, they are oxidized, and the oxidation products remove the copper oxide by complexation. The oxide layer reforms. The net result is oxidation of the carbohydrate and consumption of the copper electrode. The latter is in the form of a wire and is pushed by a constant pneumatic pressure against the face of the sample inlet tube, the terminus of which is an thin inert insulating polymer ring, separating the working electrode from the counter electrode.

Acknowledgment

This work was supported by ThermoFisher/Dionex and the Hamish Small Chair endowment at the University of Texas at Arlington. I thank Dr. Purnendu K. Dasgupta, Dr. Charles Phillip Shelor, Dr. Yongjing Chen, Dr. Chuchu Qin, Dr. Bikash Chouhan, and all other current members of the Dasgupta Research Group for their unwavering support during my time at UTA, as well as valuable insight towards the development of this research and text.

Dedication

This manuscript is dedicated to my parents Richard and Leticia Wilson, for their unending support that they have showed, and continue to show as my life progresses.

Table of Contents

List of Figures

Chapter 1

Introduction

Quantitative analysis of carbohydrates has been of vital interest in food, drug, and health related studies. In foods, carbohydrates provide information on product quality, nutritive value, state of adulteration, and general composition information;[1] carbohydrate profile in beer, for example, is often used for quality control.[2] In life sciences, the analysis of glycoproteins, glycolipids, polysaccharides, and other carbohydrates is critical.[1,3,4] Pathogens for instance are identified by carbohydrate profiling.[5] In addition to quantifying carbohydrates, differentiating carbohydrate species is also important. Only occasionally is the knowledge of the total sugar concentration suffice; the most notable example is judging readiness of grapes for harvesting: this is carried out by the measurement of the total sugar content (expressed in degrees brix, where the brix unit is essentially equivalent to the weight% sugar content in the juice), often determined in the field by a handheld refractometer.[6] Even in comparable situations with fruit juices, different sugars are typically separately determined after separation by high performance liquid chromatography (HPLC) with a universal bulk property detector such as a refractive index (RI) detector.[7,8]

Separation and Detection.

Separation and detection methods can sometimes be independent of each other but more often, the choice of the detection method may be governed by the separation method and *vice-versa.* Gas chromatography (GC), liquid chromatography (LC), and capillary electrophoresis (CE) are the only separation techniques that have been significantly used to separate carbohydrates. Gas chromatography is the most mature

of these and permits greater separation efficiencies. However, carbohydrates must first be derivatized to form volatile products to permit a GC separation. Schenk et al.[9] for example derivatized mono- , di-, and tri-saccharides via permethylation or oximation/pertrimethylsilylation and then analyzed them via the highly sensitive and nearly universal vacuum ultraviolet (VUV) absorbance detector. The VUV absorbance detector is not, however, compatible with any liquid solvents and thus HPLC.[9] Also, larger carbohydrates still cannot be converted to sufficiently volatile derivatives.[9] Most carbohydrates do not display significant UV-VIS optical absorption and are natively nonfluorescent; absorbance or fluorescence detectors cannot be used sensitively without derivatizing the analyte first. In HPLC, prior derivatization with suitable fluorogenic reagents such as 2-aminobenzoic acid[10] or 8-aminopyrene-1,3,6-trisulfonic acid[11] permits carbohydrates to be detected by fluorescence, particularly in the hydrophilic interaction mode.[10] Such fluorescence derivatization has also been used prior to CE separations.[11,12] Such prior derivatization steps, may, however, be cumbersome and laborious.[13,14]

Of universal detectors, refractive index detection is applicable but is relatively insensitive. A industry study by the Knauer corporation[15] compared electrochemical detection (ECD) and refractive index detection (RID) for glucose, arabinose, and sucrose.[15] They found that for glucose and arabinose, that the sensitivity of ECD was around 5000 times higher than that for RID, and 1000 times higher for sucrose.[15] Additionally, it is important to note that the use of organic solvents such as acetonitrile can significantly increase routine cost of analysis.[16] Carbohydrates are also nonvolatile, this has led, however, to the use of detectors that evaporate the solvent completely and

then detect the residual solute, now present as aerosol particles.[10,17] In particular, evaporative light scattering and charged aerosol detection (CAD) have been used after HPLC separation of carbohydrates.[18,19] The use of evaporative detectors such as the CAD, however, preclude the ability to put any nonvolatile substances such as buffering agents in the eluent, thereby imposing stringent limitations on the eluent composition. The same is true of mass spectrometry (MS), with or without prior HPLC separation, although MS can be a singularly powerful and sensitive tool in solving complex problems.[20,21] Zygler et al.[22] analyzed commercial artificial sweeteners found in yogurt, fruit juices, sugar-free drinks, and fish products using HPLC-MS. While MS was able to determine each individual sweetener, the downside of this method was the lengthy derivatization process to account for analysis by MS.[22]

High Performance Anion Exchange Chromatography and Pulsed Amperometric Detection (HPAE-PAD).

For any analysis, a detection method that does not require any derivatization or pretreatment, and that can be coupled to gradient elution HPLC to separate complex mixtures of multiple mono- or oligosaccharides is preferred. Anion exchange chromatography meets these separation requirements and also does not require the use of organic solvents, and PAD is not only sensitive, but it does also not need time-consuming derivatization steps, and is thus very simple to use.[3,23–25]

Innovation in the analysis of carbohydrates became an intense area of activity in the 1980's. Pohl et al. demonstrated the analysis of a variety of aldoses, ketoses, and other polysaccharides via HPAE-PAD using a gold electrode.[26] They demonstrated a high-performance separation method for carbohydrates with excellent limit(s) of

detection (LOD).[26] Further, with judicious choice of the eluent gradient, the retention order of different carbohydrates could be altered; this was not previously possible.[27] When DC amperometry is used, the electrode gets fouled with the oxidation products and loses sensitivity quickly. On the other hand, PAD uses a continuously repeated waveform, with a minimum of three voltage steps that ideally regenerate a clean gold surface after each cycle.[26] For carbohydrate determination, such a triple voltage waveform was used, the potential of the working electrode (stated with reference to a Ag/AgCl electrode) was set to step between -0.8 V (240 ms), 0.2 V (60 ms), and then 0.6 V (60 ms), with a total cycle time of 360 ms.[26] The initial step reduces any gold oxide back to gold, then the carbohydrate oxidation current is measured at 0.2 V, and finally any adherent oxidation product is burned off at the high positive potential step of 0.6 V (cleaning step), in this step some of the electrode surface may be oxidized to gold oxide.[26] The oxidation of the carbohydrate analyte reliably occurs and the oxidation current (typically in nanoamperes, nA) can be reliably measured only when the gold electrode surface is clean and is not covered with other adsorbed products or gold oxide.[26,28] Johnson et al. further improved the robustness of PAD in so it could be routinely used in conjunction with HPAE chromatography for carbohydrate analysis.[29,30]

Electrode fouling is common in electrochemical detection where the analyte or electrode oxidation product is not completely removed from the active electrode surface and steadily reduces the signal of the observed analyte.[3,29–32] Either the high potential oxidation step is not completely effective in removing all the analyte oxidation products (during this step gold oxide is formed on the electrode) or the reduction step used in the protocol is not entirely efficient at reducing the gold oxide formed, the surface slowly

degrades from being pure metallic gold in the measurement step.[26,29] The metal oxide can also result in dissolution of the oxide into the eluent.[26,29] After an electrode has been fouled, it must be removed from the system and repolished and the system recalibrated.[26,29,33] Development of disposable electrodes containing evaporated metal on a plastic film permits rapid replacement, but high accuracy work will still typically require recalibration after replacement.[33,34]

Gold and platinum electrodes are the most widely used electrodes in analytical electrochemistry.[35] In general, platinum electrodes are more widely used in electrochemistry than gold because of the higher potentials that can be used, but the electrochemical oxidation of carbohydrates is a catalytic process and it proceeds much faster on a gold surface, thus providing far greater sensitivity. However, gold itself oxidizes under positive potentials much more easily, especially at alkaline pH.[35] Copper electrodes are consumed in electrochemical processes but can be otherwise attractive.[36] For amino acids, Kok *et al.* compared amperometric detection with several common HPLC detection methods.[37] They found it exhibited a similar or better LOD when compared to ultraviolet (UV) absorbance detection after derivatization, visible absorbance detection after ninhydrin reaction, fluorescence detection after *o*-phthalaldehyde (OPA) reaction, and potentiometry with a copper electrode.[37–43] Ueda *et al.* investigated attainable LODs for glucose with constant-potential amperometric detection, individually on Cu, Rh, Cu-Ni, Ni, Co, Ag, Ir, Pd, and Fe, all in the form of 1-mm dia. electrodes.[44] The LOD ranged from 0.22 pmol on a copper electrode to 60.0 pmol on an iron electrode.[44] Similar LODs were reported for a variety of carbohydrates, sugar acids, and alditols. Typically gold is preferred over copper in an oxidative

detection process because gold oxidizes at a higher potential than copper, permitting the use of a higher potential for detection.[45,46] However, an oxide layer forms more easily at higher potentials and for most metals, the development of a oxide layer eventually leads to an impermeable insulating coating.[3,18,26,29,45,46] For copper though, the oxide may be (electrochemically) more active than the bare metal.[45,46]

In summary, there is still a clear need for a more robust detection system for chromatographic analysis of carbohydrates. Recognizing the finite number of available metals, and their limitations and the limitations of PAD itself to completely rejuvenate a surface, we introduce here a new concept for a feed-through electrode, that is deliberately used in a mode wherein the surface is consumed, which continually renews the surface. This concept is demonstrated in the constant potential amperometric mode using a copper electrode. In contrast to all previous work, oxidative dissolution of the electrode is welcome; the electrode is continuously advanced under constant pneumatic pressure to maintain the same interelectrode gap and sensitivity.

Chapter 2

Experimental

Materials.

99.9% Glucose (Mallinkrodt Inc.), 99.9% fructose (J.T. Baker), 99.9% sucrose (Fisher Scientific) were obtained as indicated above. High purity deionized (DI) water, supplied by an Aries water purification system, was used to prepare all solutions. Sample solutions were filtered through Versapor Membrane Acrodisc syringe filters, (5 μm pores, 25 mm, Pall.com) or PTFE membrane syringe filters (0.22 μm, 13 mm, VWR International) prior to injection.

Carbohydrate Selection and Preparation.

Each carbohydrate was first dissolved in water to make a stock concentration of 10 g/L. The stock solution was stored refrigerated. Each of these were then diluted serially to 1000, 100, and 10 ppm (mg/L) concentrations. A mixture of the three carbohydrates (100 ppm concentration each) was prepared by pipetting 25 mL each of the three 1000-ppm stock solutions into a 250-mL volumetric flask and diluting to volume. A 100-ppm mixed standard was created from this secondary stock daily by 10-fold dilution. All analyte solutions were preserved by spiking with sodium azide to achieve a concentration of 10 ppm.

HPAE Instrumentation and Conditions.

Carbohydrates were separated by anion exchange chromatography with electrochemical detection at a copper electrode. A Thermo/Dionex ICS-5000 with dual pumps (one analytical scale, one capillary scale) and dual eluent generators (KOH and

methanesulfonic acid) was used to produce a mixture of KOH and potassium methanesulfonate (KMSA). The chromatographic flow path is depicted in Figure 1. Deionized water is pumped by the analytical scale pump at a flow rate of 0.060 mL/min and split between the KOH and MSA eluent generators using chromatographic tees and equal lengths of 0.005” i.d. polyetheretherketone (PEEK) tubing, to obtain approximately equal flows through the individual generators. The separate streams are then recombined through another tee before going to a degasser to remove electrolytic gases. Because the eluents are electrodialytically regenerated and then recombined, the exact flow through each generator has no effect. The stream then flows through a 400 nL internal loop injector, a CarboPac PA200 guard (0.4x50 mm) and separator (1x250 mm) column set, detector, and a pH reference electrode. The injector and column are maintained at 30 °C. The electronics of an ICS-5000 electrochemical detector module (P/N 072043) and a combination pH and Ag/AgCl reference electrode; are used with the custom electrode. System control and data acquisition was performed using Chromeleon V7.2 software. All of the above were from Thermo Fisher Scientific/ Dionex, Sunnyvale, CA.

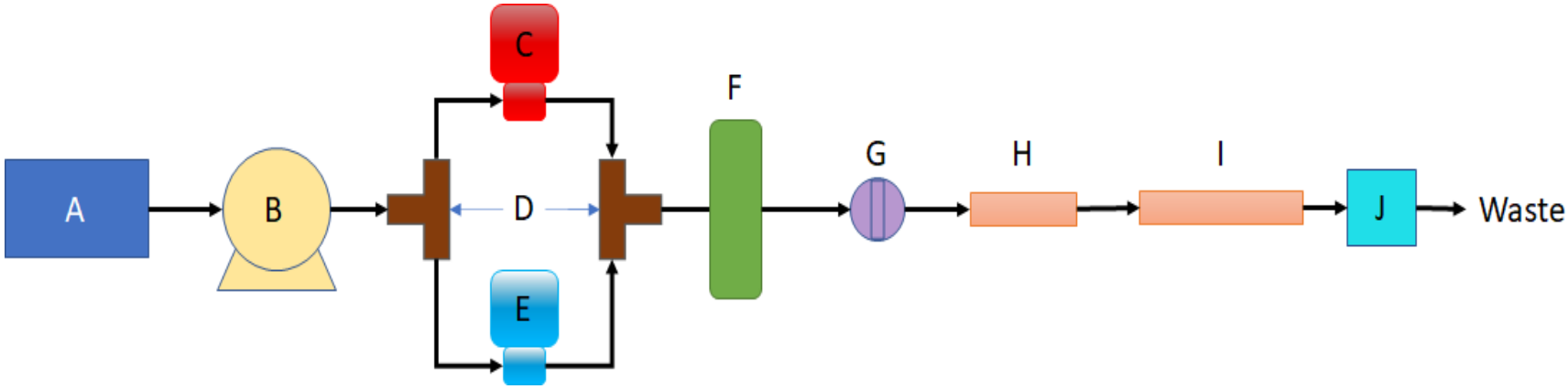

Figure 1. Schematic of chromatography system. **A**: High purity deionized water source. **B**: Analytical pump, 0.050 mL/min, 30 °C. **C**: KOH Eluent Generator (EG), **D**: Tee setup to split and recombine the flow to/from the eluent generators **E**: MSA Eluent Generator. **F**: Degasser to removing O_2 and H_2. **G**: 4-port 400 nL injection valve. **H**: Guard column. **I**: Separator column. **J**: Present electrochemical detector with a copper electrode.

Preparation of the Copper Electrode.

Prior conditioning of the electrode is necessary for detection to take place. Ideally, the conditioning procedure initially should start with freshly polished copper. If the copper wire has been conditioned once previously or is suspected to have impurities, a negative voltage can be applied to remove any copper oxide from the surface, and then re-form a reproducible copper oxide layer which is needed for reproducible detection. With pH as the reference electrode, a typical reconditioning process first removes the oxide layer (if necessary) by stepping from 0 to -0.5 V every 0.1 V every 20 minutes. The potential is then stepped up to 0.4 V by 0.1 V every 20 minutes, at which point the potential remains at 0.4 V for $\geq$ 1 hour. This is followed by a 0.1 V step every 30 minutes going up to 1.3 V. Typically, the electrode is maintained at this potential overnight to allow the formation of a robust copper oxide layer. The oxidation current is initially high, but as the oxide layer is formed the current decays until a stable baseline is formed. The voltage is then stepped down by 0.05 V every 20 minutes until 0.95 V. The system is then allowed to go to equilibrium.

Design of a Continuously Renewable Copper Electrode.

The construction of the self-advancing electrochemical detector is shown schematically in Figure 2. All connections were made with standard ¼-28 flat bottom compression fittings and obtained from IDEX Health Sciences (www.idex-hs.com). The inset shows an expanded view of the detector cell geometry in a wall jet configuration where fluid impinges on the copper working electrode. Fluid enters from a 125 µm I.D. x 1/16” inch O.D. stainless-steel tube (SS) which also serves as the counter electrode. A ~1 mm long (125 µm I.D. x 1/16” inch O.D.) ethylene-trifluoroethylene (ETFE, Tefzel®) tube

serves as an insulating spacer between the SS tube and the 330 µm copper wire (CW, MWS Wire Industries, P/N EY71287-1) working electrode. The CW is introduced from the opposite side through a 360 µm I.D x 1/16” inch O.D. PTFE jacket tube and pierces through a 1/16” inch thick silicone septum. The CW and jacket tube, SS tube, insulating spacer, and silicone septum are all aligned by insertion into a 1/16” I.D. x 1/8” O.D. PTFE tube. This larger alignment tube contains a 0.91 mm diameter hole drilled into the wall to allow liquid to escape. The components are inserted into the alignment tube until the septum and spacer interface are aligned with the exit hole leading to the reference electrode. The alignment tube is then inserted through a ETFE (original I.D. 0.005”) tee bored out to 1/8” in the horizontal direction to allow passage of the tube. The ferrules and nuts form the seal and hold the various components in place.

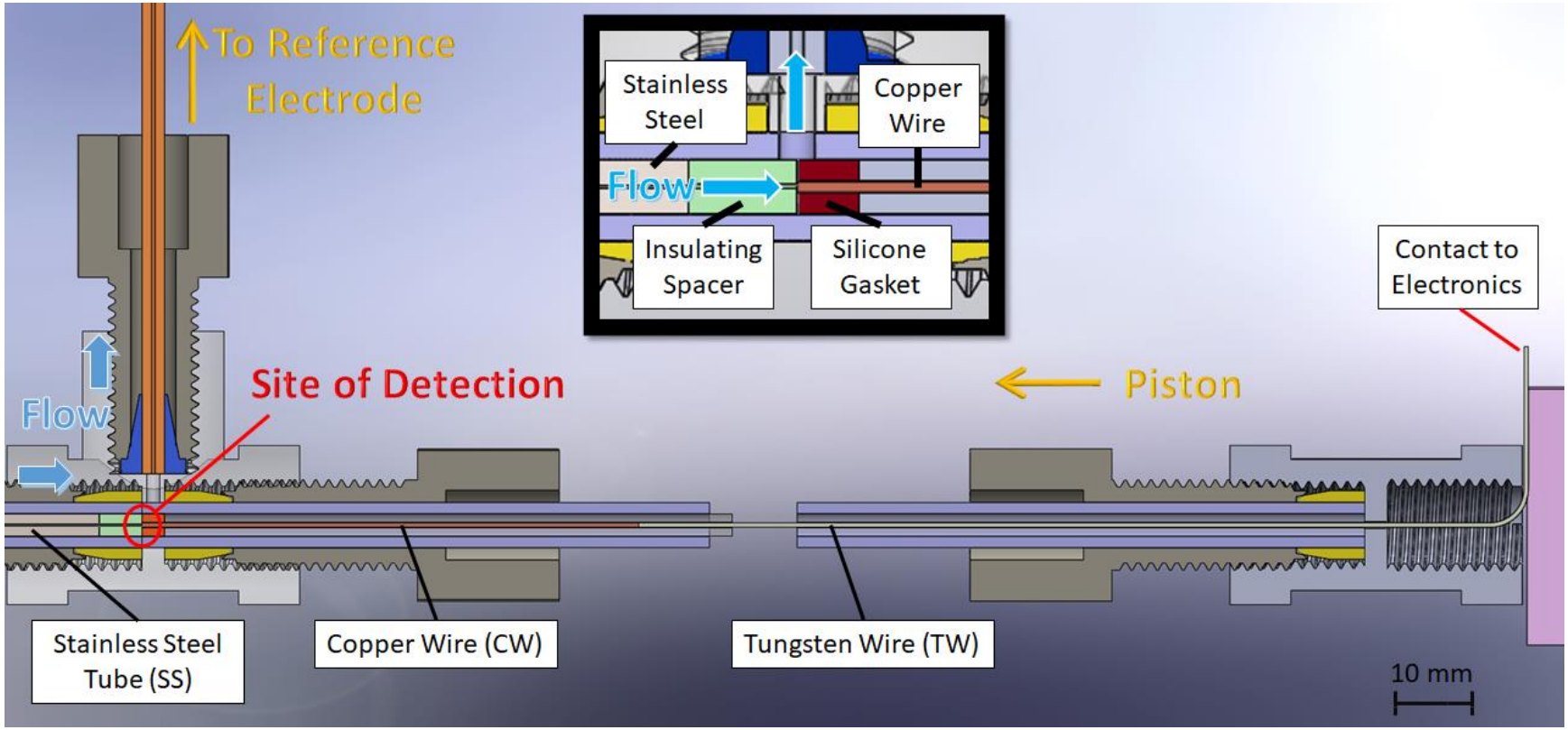

Figure 2. Electrochemical detector design. The piston is pushed by a 5 mL syringe plunger pneumatically pressurized to 3-6 psi which forces the tungsten wire to contact the Cu wire with a force of and advances it as it undergoes dissolution. The stainless steel tube and tungsten wire form the counter electrode and working electrode contacts, respectively for the detector electronics. **SS**: 125 µm I.D. x 1/16" inch O.D. stainless-steel tube, length: 79 mm. **CW**: 330 µm copper wire. **TW**: 300 µm Tungsten Wire.

As the CW dissolves, it is advanced by a pneumatic piston as shown in the right-hand side of Figure 2. A 300 µm diameter tungsten wire (TW) is inserted through nested 360 µm I.D. x 1/16” O.D. and 1/16” I.D. x 1/8” O.D. PTFE tubing as was done for the copper wire. The jacket tubes provide mechanical support for the TW which travels through the union and is bent at the opposite side to allow for contact with the detector electronics. A styrofoam pad is inserted after the union and bent TW and is pushed upon by the plunger of a 5 mL syringe (not shown in figure) seen in Figure 3. The syringe is connected to a pressure regulator that delivers 3-6 psi for ~0.5 – 1.0 lbs of force or ~7 - 14 kpsi pressure at the distal tip of the tungsten wire. The tungsten wire is cut to allow 9 mm to protrude from the PTFE tubing and polished to remove any burrs. The distal tip of the tungsten wire contacts the copper wire which is slightly recessed in its jacket tubing as seen in Figure 2. The whole arrangement is affixed to an acrylic block with cable ties that permit motion of the syringe plunger/TW/CW assembly in the horizontal direction of Figure 3.

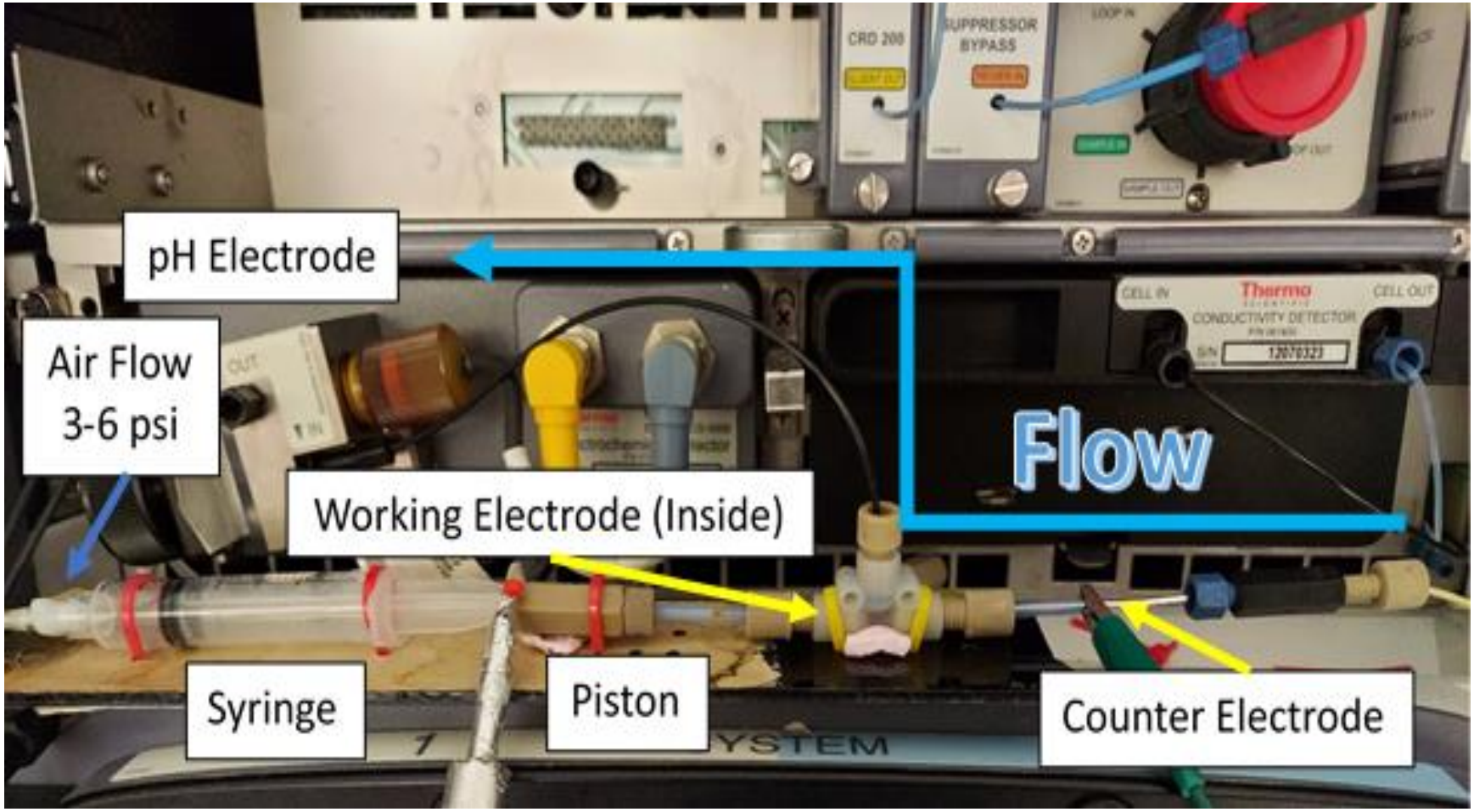

Figure 3. Physical layout of detector. The piston is free to move in the horizontal direction and is advanced by the plunger of syringe connected to a regulated pressure source. The ICS-5000 electrochemical detector electronics are connected to the tungsten wire and SS inlet tube as the working electrode and counter electrode, respectively. Eluent flows through the SS tube into the detector and in its exit path contacts the pH reference electrode. The pressure regulator for the air flow is downstream of the connection on the syringe tip, not visible in the photo.

Chapter 3

Results and Discussion

Degradation of Gold Electrode

DC amperometry with a gold electrode above or near the oxidation potential was carried out to see the effect of signal decay. Figure 4 shows peak height as a function of injection number and time for three analytes, glucose, fructose, and sucrose at a concentration of 100 ppm. Glucose, fructose, and sucrose were analyzed with DC amperometry using a commercial non-disposable gold electrode, using an applied potential of 0.2 V vs. Ag/AgCl electrode as the reference electrode. Prior to analysis the system was allowed to run under a pulsed waveform to electrochemically remove any impurities or gold oxide on the gold surface. Presumably, the gold surface was contaminant free when injections began. Of the three analytes, the best performing analyte was glucose which lost over half of its signal after 18 injections, or about 3 hours as each injection had a 10-minute duration. The other two analytes, fructose, and sucrose were even more rapid respectively losing over half of their signal in 6 and 3 injections. At some point, sucrose lost so much of its signal that the software could no longer detect the analyte. Even manual integration of peak could not occur at this point either as the peak was no longer visible on the chromatogram. This rapid loss of signal indicates the ready formation of a gold oxide surface when operating under DC conditions. This is concurrent with the work on platinum electrodes done by Manica *et al.*[47] where they had observed that there signal would decay by 80-90% after 10 runs. Various authors have noted that fouling of gold electrodes can occur during HPAE-PAD detection of carbohydrates or other analytes, and to counteract such fouling measures

such as polishing or a pulsed waveform would have be used to mitigate this effect.[3,26,29] This in turn necessitated the use and development of gold disposable electrodes[33,34] or a viable alternative to maintain an analyte's signal intensity for routine analysis. Additionally, inset in Figure 4 the 1st, 50th and 100th chromatograms are shown together to illustrate the degree of signal decay as more injections occurred. The analytes eluted in order are glucose (R = 2.84), fructose (R = 3.21), and sucrose (R = 3.60). After 50 injections, all analytes showed significant decay, with sucrose being almost eliminated from detection.

Pulsed Amperometry.

High performance ion exchange chromatography with pulsed amperometric detection, however, can provide superb separation and detection. Figures 5 and 6 shows a separation of inulin, a prebiotic from chicory root, under somewhat different gradient conditions. The steeper gradient in Figure 6 seems to allow for more complete separation of the analyte by increasing elution of the analyte off the column. Additionally, peak height is increased as compared to the gentler gradient in Figure 5 which suggests the efficiency of the separation is better under more aggressive conditions.

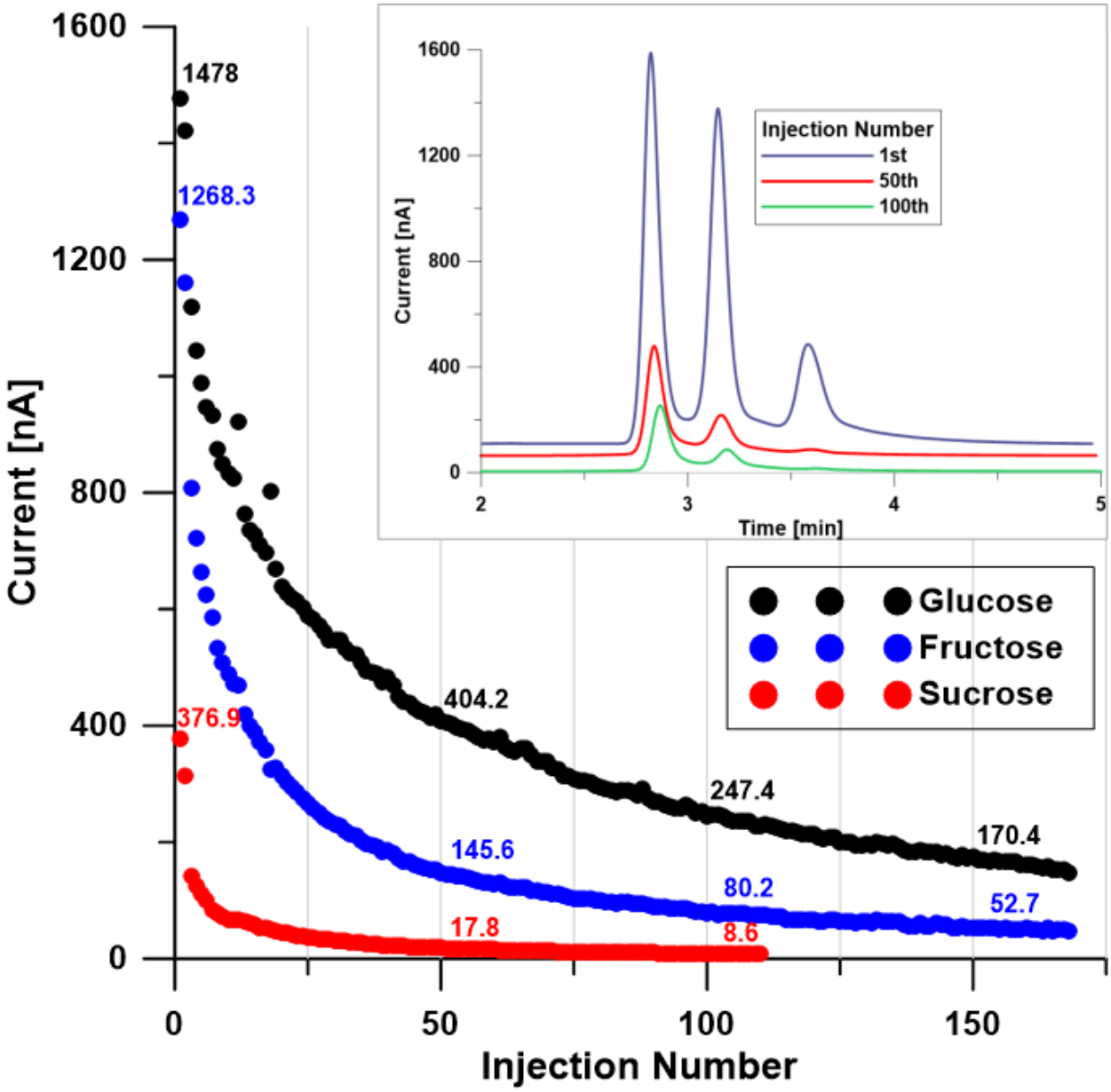

Figure 4. Signal decay at a gold electrode using DC Amperometry at 0.2 V vs Ag/AgCl. Analytes are 100 ppm each separated using 60 mM KOH. The inset shows select chromatograms during the electrode aging. Flow Rate: 63 μL/min. Injection Volume: 400 nL. Eluent Concentration: 60 mM KOH. Column Temperature: 35 °C. Electrochemical Detector settings: DC voltage, 0.2 V; data collection frequency, 20 Hz; rise time, 0.50 s. Reference Electrode: pH

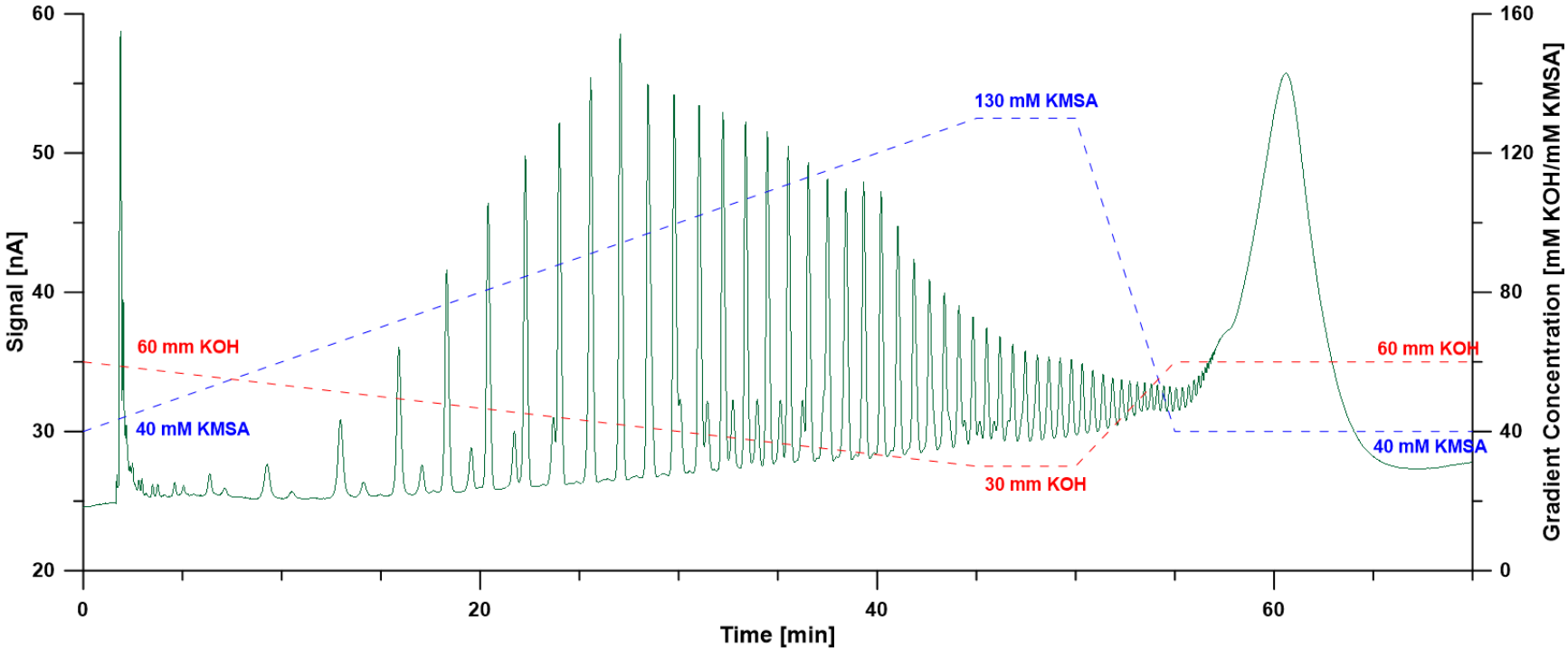

Figure 5. Separation of Inulin prebiotic from chicory root. Pulsed amperometry using a gold electrode with an Ag/AgCl reference electrode was used to separate the analyte. Column: 1 mm x 250 mm Dionex CarboPAC PA200 column, particle size: 5, functional group: Quaternary Ammonium Functionalized Latex. Analyte Concentration: 5000 ppm. Flow Rate: 63 μL/min. Injection Volume: 400 nL. Gradient: 40 mM KMSA/60 mM KOH to 130 mM KMSA/30 mM KOH during 0-45 min, 130 mM KMSA/30 mM KOH during 45-50 min, re-equilibration during 50-65 min; Column Temperature: 35 °C. Electrochemical Detector settings: E1: 0.1 V (400 ms), E2: -2.0 V (20 ms) E3: 0.6 V (20 ms) E4: -0.1 V (60 ms); data collection frequency, 2 Hz.

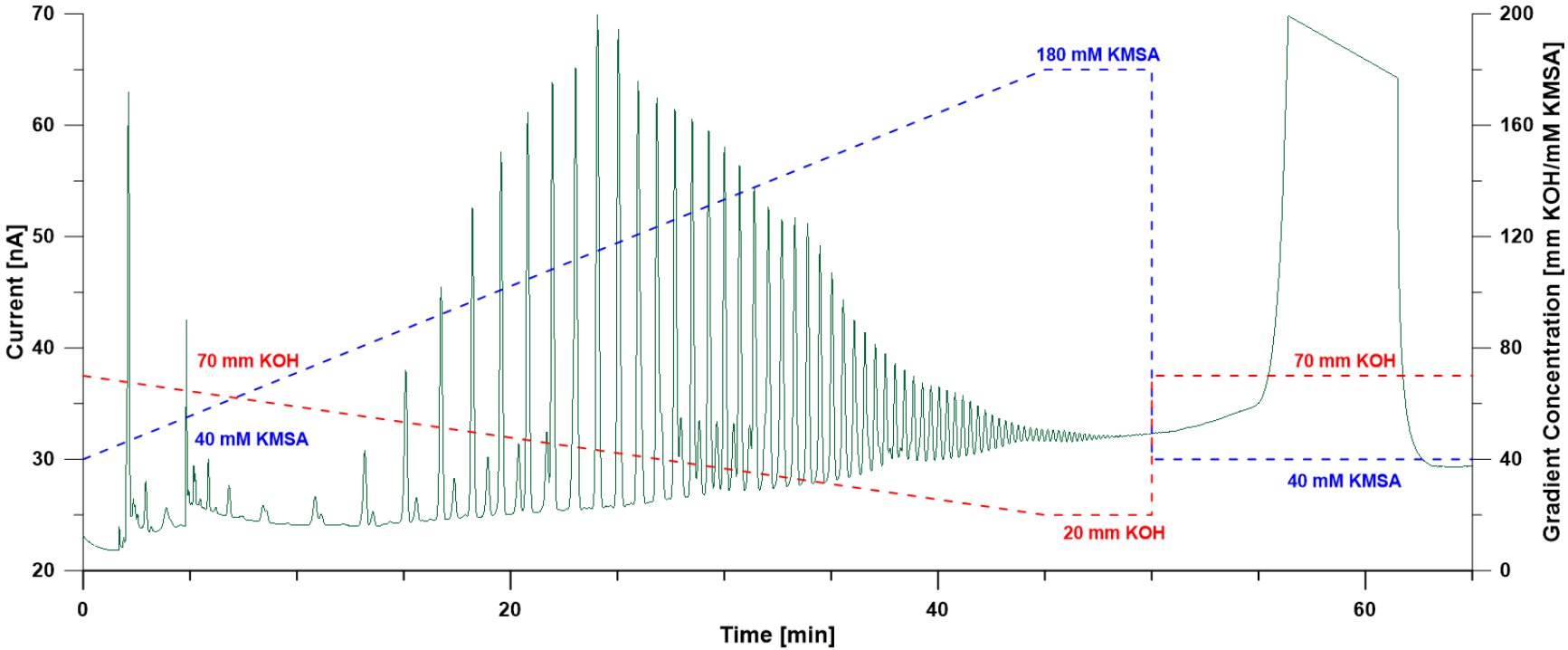

Figure 6. Separation of inulin prebiotic from chicory root. Pulsed amperometry using a gold electrode with an Ag/AgCl reference electrode was used to separate the analyte. Gradient: 40 mM KMSA/70 mM KOH to 180 mM KMSA/20 mM KOH during 0-45 min, 180 mM KMSA/20 mM KOH during 45-50 min, re-equilibration during 50-65 min. Other conditions same as in Figure 5.

Mechanism of Electrochemical Detection.

Under strongly alkaline conditions, at least one of the -OH groups in a carbohydrate ionize, forming the corresponding anion. If in proximity to an Au or Cu electrode held at a sufficiently positive potential, the anion can be oxidized, most often to a carboxylic acid. At the potentials necessary for carbohydrate oxidation, the metals themselves can oxidize to a degree and an oxide layer forms at the metal surface. The standard oxidation potential of Cu and Au are 0.34, and 1.83 V, respectively.[35] Oxide formation is thus obviously more facile for copper than gold. For this reason, gold is often the electrode of choice as it provides the best combination of sensitivity and longevity.[3,26,32,37] The oxidation mechanism is not well understood for a copper electrode. It has been proposed that in strongly alkaline medium some Cu(III) oxide CuO(OH), maybe formed from the CuO present. This oxidizes the nucleophilic carbohydrate anion forming a radical intermediate and regenerating CuO. The radical intermediate then decomposes to the final product.[44] The carbohydrate anion and/or the oxidized products may also chelate the cationic metal resulting in gradual loss of the electrode surface.[48] The mechanism due to Fleishmann et al,[49] as advocated by Ueda et al.[44] for oxidation of a carbohydrate at an electroactive copper oxide surface, is as follows:

$$OH^- + Cu\ (II) \overset{k_e}{\Leftrightarrow} Cu\ (III) + H_2O + e \quad (1)$$

$$Cu\ (III) + Carbohydrate \xrightarrow{k_C,\ rate\ determining\ step} Cu\ (II) + radical\ intermediate \quad (2)$$

$$radical\ intermediate + Cu(0) \rightarrow copper - carbohydrate\ complex + (n-1)e \quad (3)$$

Overall, this will expose a fresh copper surface which will undergo oxidation to reform the oxide layer.[44] It should also be noted that in highly alkaline media, the hydroxo

copper ion, cuprate, $[Cu(OH)_4]^{2-}$, may increasingly form and contribute to the loss of the electrode material.[50] While this may lead to an elevated background current but it also produces a fresh electrode surface.[50] The works of Striegler and Tewes,[51] Cerchiaro et al.,[52] Marioli et al.,[36] suggest that the alkoxide on the anomeric carbon of the carbohydrate plays a major role during this complexation, at least in the case of simple sugars. The 1,2-enediol formation of the sugar is suggested to have a major role in formation of the copper-carbohydrate complex, and has a direct relationship with the oxidation rate of carbohydrates.[36,52] Marioli et al.[36] conducted cyclic voltammograms of glucose related compounds in alkaline solution using a rotating ring disk electrode. They noted the oxidation of glucose is catalyzed by Cu (III) species after the adsorption step.[36] Furthermore, the complexation process goes past a two-electron transfer which normally leads to gluconic acid, this suggests Cu(III) involvement.[36] Complexing sites to copper is generally prioritized as follows: a cis-diol in a five-membered ring > a cis-diol in a six-membered ring > a trans-diol in a six-membered ring.[52] The presumed coordination sites for formation of the complex include the cis-diol as present in glucose at the anomeric C1 and adjacent C2, and the bond between the anomeric C1 and the adjacent O5 oxygen which is in agreement with work done by Marioli.[36,51,52] It is also understood that the mechanism may be different for reducing and non-reducing sugars.[52,53] The mechanism for a reducing sugar likely centers on the oxidation of the sugar itself as a first step.[52,53]

Optimization of Operating Conditions.

Preliminary studies suggested that the optimal working potential be above 0.90 V vs. the pH electrode for 60 mM KOH as eluent. An ideal potential would be one in which all

analytes are baseline resolved from one another. A mixture of glucose, fructose, and sucrose, 100 ppm each, were carried out at applied potentials from 0.90 V to 1.20 V vs. the pH electrode in 0.05 V steps to gauge signal response. Figure 7 shows the peak heights of the three analytes as a function of the applied voltage. They behave differently: fructose shows little dependence on the applied voltage in the range studied, while glucose has the highest response at the lowest applied voltage, goes through a minimum at an applied voltage (V_{app}) of 1.05 V and then rises again. However, overall, all these values are within ±~5% from the average response. In contrast, the response to sucrose, much lower than the two reducing sugars, rises monotonically until an applied potential of 1.10 V is reached and then reaches a plateau.

Figure 8 shows the background current, the noise associated with the background and the S/N ratio (SNR) for each analyte as a function of the potential. The noise current essentially remains constant until the background current reaches 35.27 ± 0.89 nA, then rises steeply. A plot of the noise current vs, the background current shown in Figure 9 shows that the noise does have a square root dependence on the background, i.e., the noise is not intrinsic to the current measurement process but some constant amount is being picked up in the largely unshielded arrangement. As to SNR, the highest SNR for all analytes was observed at the lowest V_{app} in the range studied. However, while the SNR decreased relatively steeply with increasing V_{app} for glucose and fructose, it remained essentially invariant for sucrose until a V_{app} of 1.10 V.

Figure 10 suggests that detector voltage settings can affect apparent chromatographic efficiency, the peaks decidedly tail more at lower operating potentials, possibly due to incomplete oxidation resulting from slower oxidation kinetics. Assuming

the proposed rate-determining step in Fleischmann et al's mechanism[36,44,49] is correct, then the kinetics of this rate-determining step could be dependent on the applied potential.[36] In such detection processes then, the applied potential can not only determine the signal amplitude, it can also affect the apparent chromatographic performance.

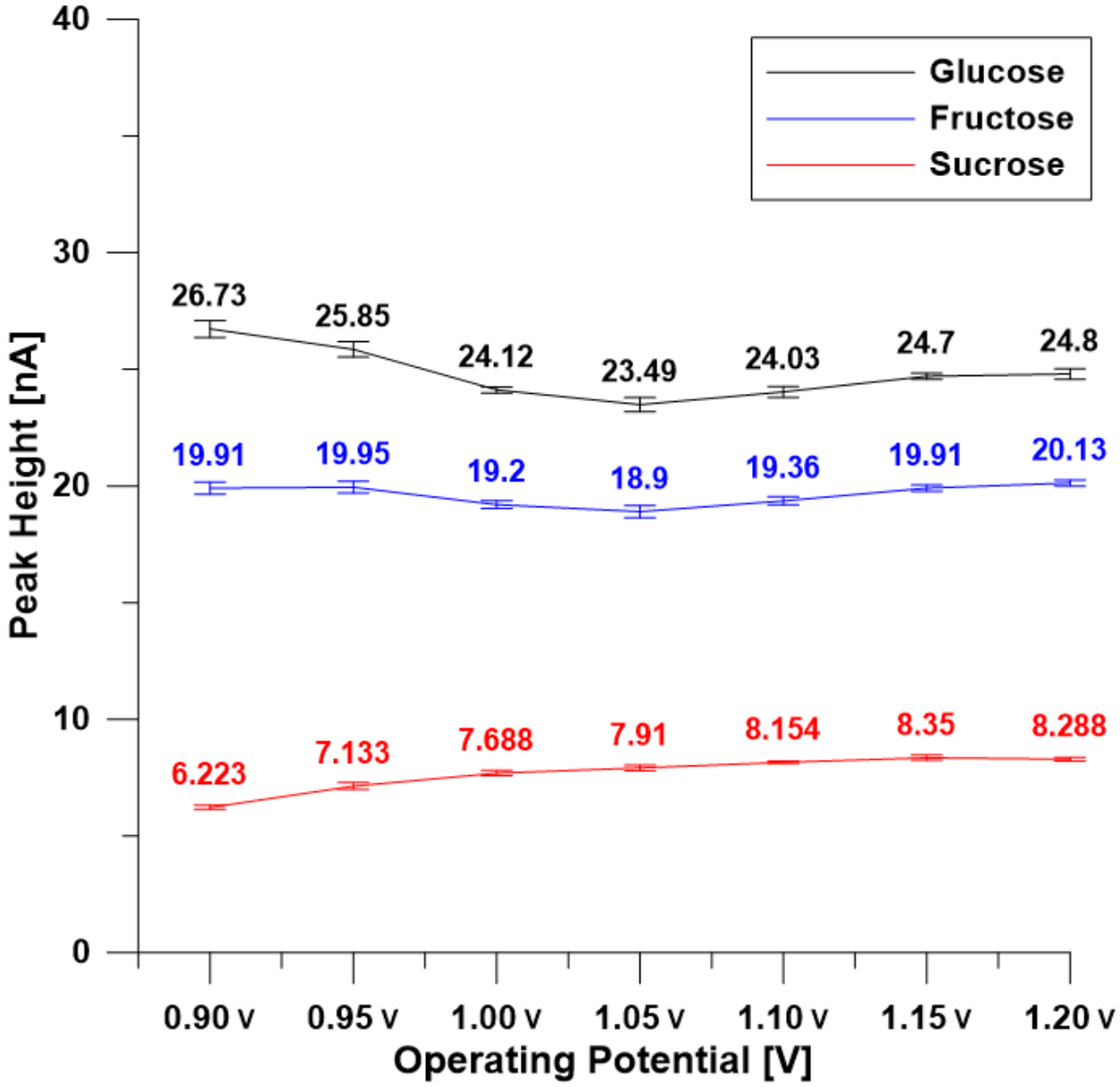

Figure 7. Peak height with increasing operating potential. Analytes: mixture of glucose, fructose, and sucrose. Operating potentials are changed from 0.900 V to 1.200 V, every 0.050 V. Column: 1 mm x 250 mm Dionex CarboPAC PA200 column, particle size: 5, functional group: Quaternary Ammonium Functionalized Latex. Analyte Concentration: 100 ppm each. Flow Rate: 50 µL/min. Injection Volume: 400 nL. Eluent Concentration: 60 mM KOH. Column Temperature: 30 °C. Electrochemical Detector settings: voltage, 0.900 V – 1.200 V; data collection frequency, 20 Hz; rise time, 0.50 s. Piston Pressure: 14 psi.

Glucose and fructose peak height as seen in Figure 7 seem to be independent of voltage, while sucrose peak height appears to have a dependence with increasing operating potential. The higher signal for glucose and fructose relative to sucrose may be that they are monosaccharides and reducing sugars while sucrose is a nonreducing disaccharide that is harder to oxidize. It is possible that the increased size of the molecule or the nature of the glycosidic bond leads to this dependence. One notes that the sucrose molecule is unique among the common disaccharides in having an α-1,β-2-glycosidic (head-to-head) linkage. Because this glycosidic linkage is formed by the -OH group on the anomeric carbon of α-D-glucose and the -OH group on the anomeric carbon of β-D-fructose, it ties up the anomeric carbons of both glucose and fructose. Additional studies with other analytes would need to be carried out to explore this behavior in greater detail.

Signal-to-noise ratios for all analytes decrease while the background current increases as the operating potential is increased (Figure 8). This arises primarily from a change in the noise levels rather than changes in the signal. The noise to background ratio decreases exponentially with increasing background current (Figure 9). A detailed analysis of the noise current and background current indicates that the noise has a background-independent component calculated at 40 pA that likely arises from poor shielding of the cell and the connecting cables. But the additional noise shows a shot-noise dependence where the additional noise is dependent linearly to the square root of the background current (Figure 10).

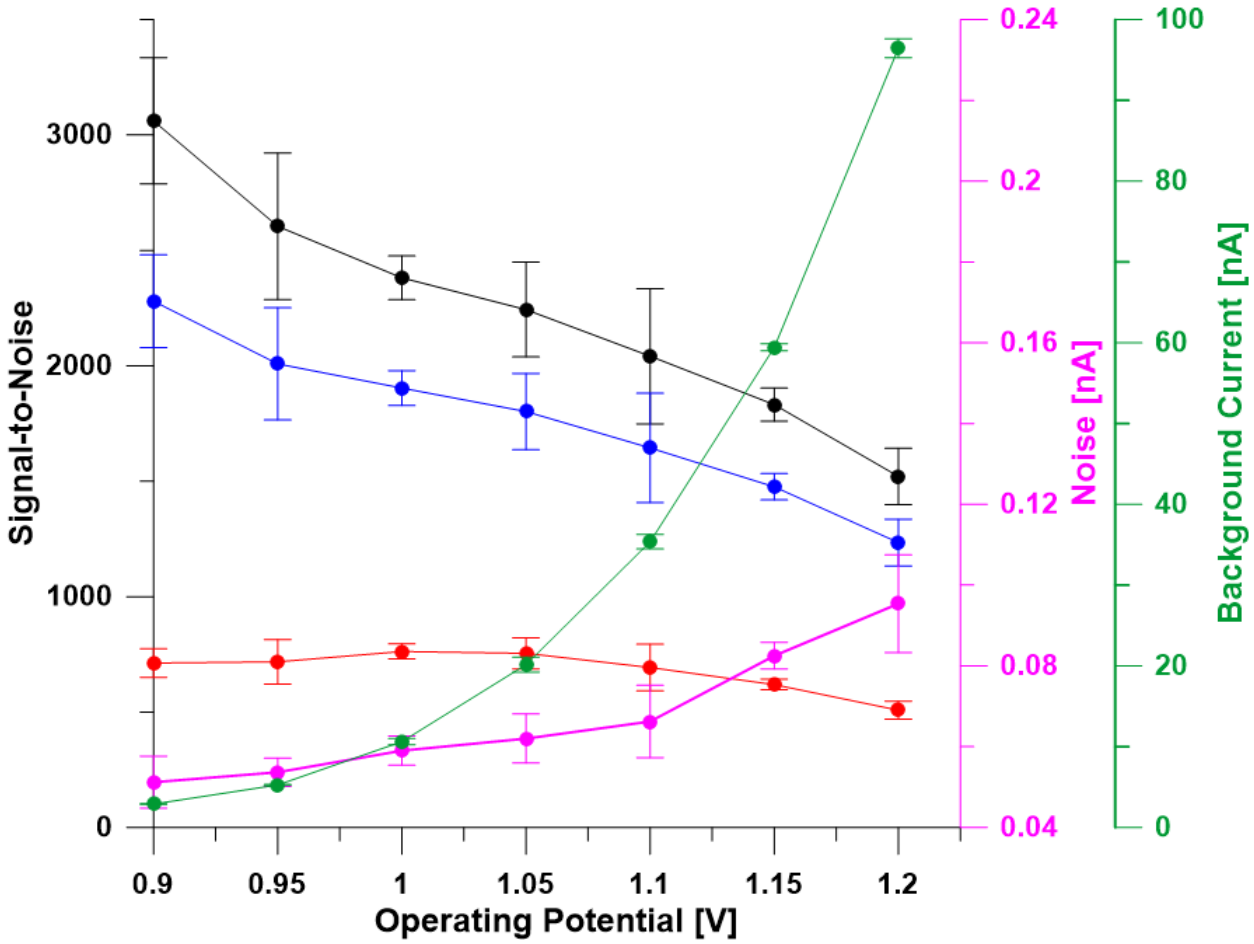

Figure 8. Signal-to-Noise and Noise with increasing operating potential. Isocratic injections of a mixture of glucose, fructose, and sucrose, 100 ppm each. Operating potentials are changed from 0.900 V to 1.200 V, every 0.050 V. Other conditions same as in Figure 7.

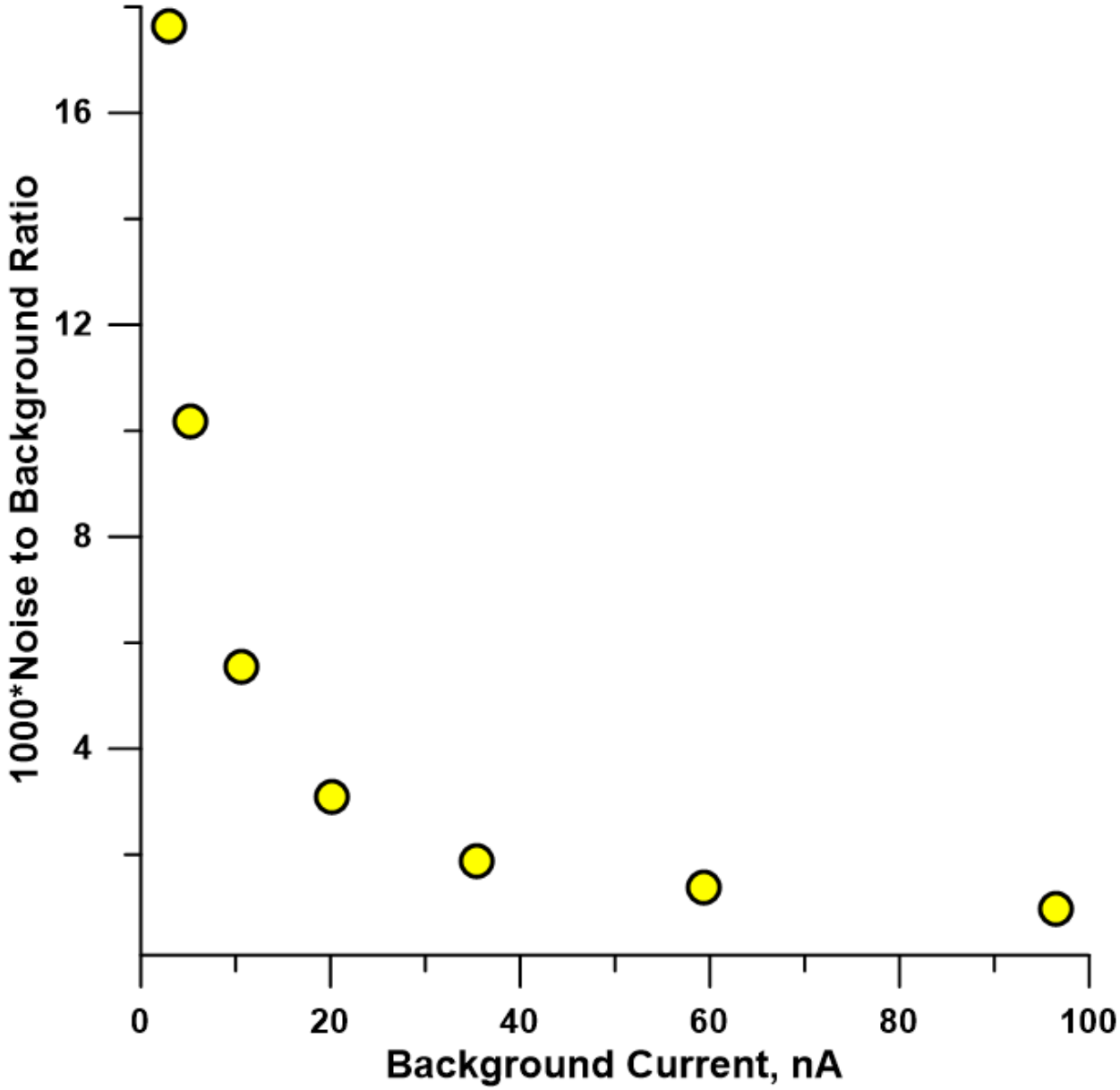

Figure 9. Noise to background ratio deceases exponentially with increasing Background current. Isocratic injections of a mixture of glucose, fructose, and sucrose, 100 ppm each. Other conditions same as in Figure 7.

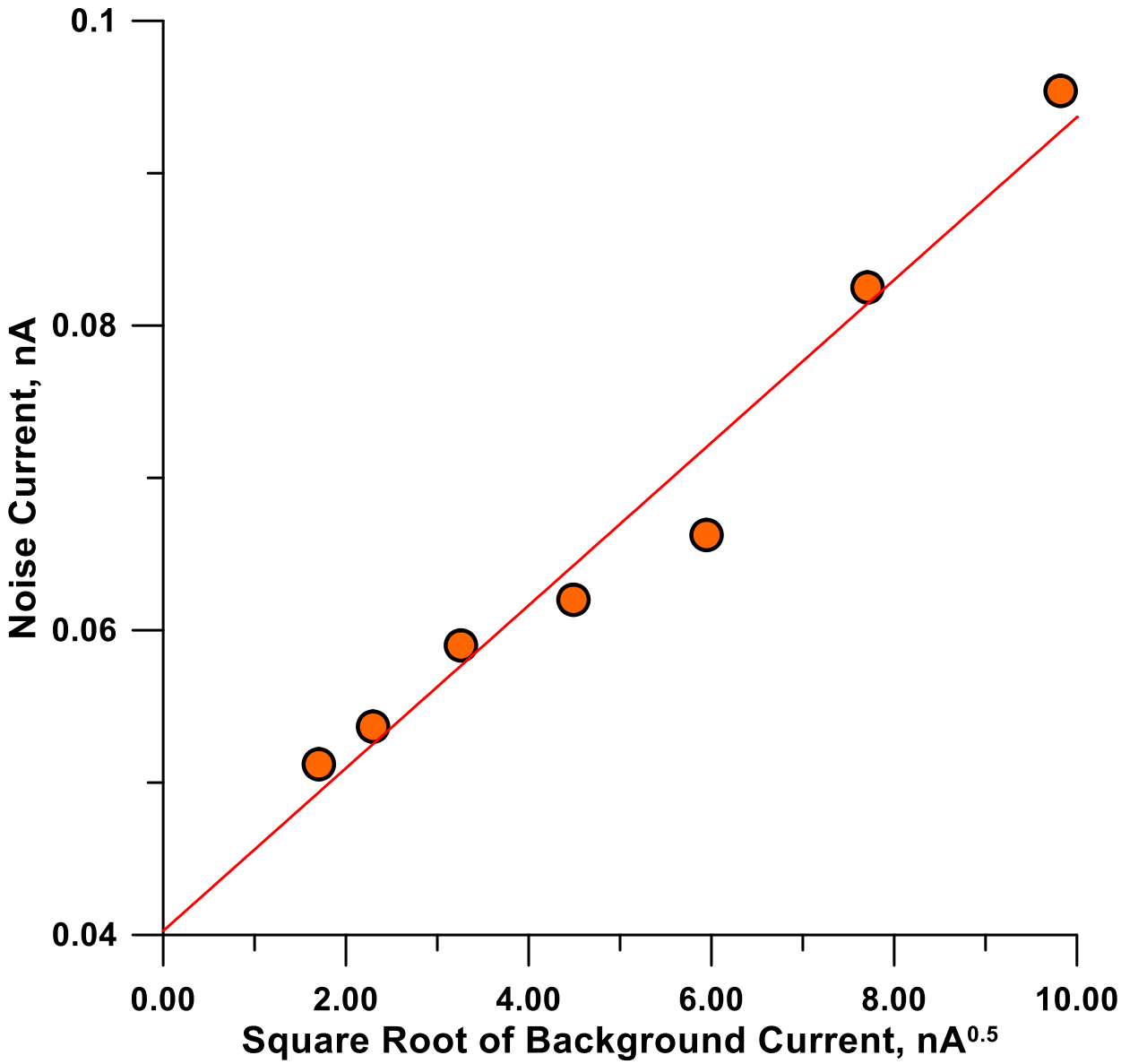

Figure 10. The noise is linearly proportional to the square root of the background current with an background-independent component of ~40 nA.

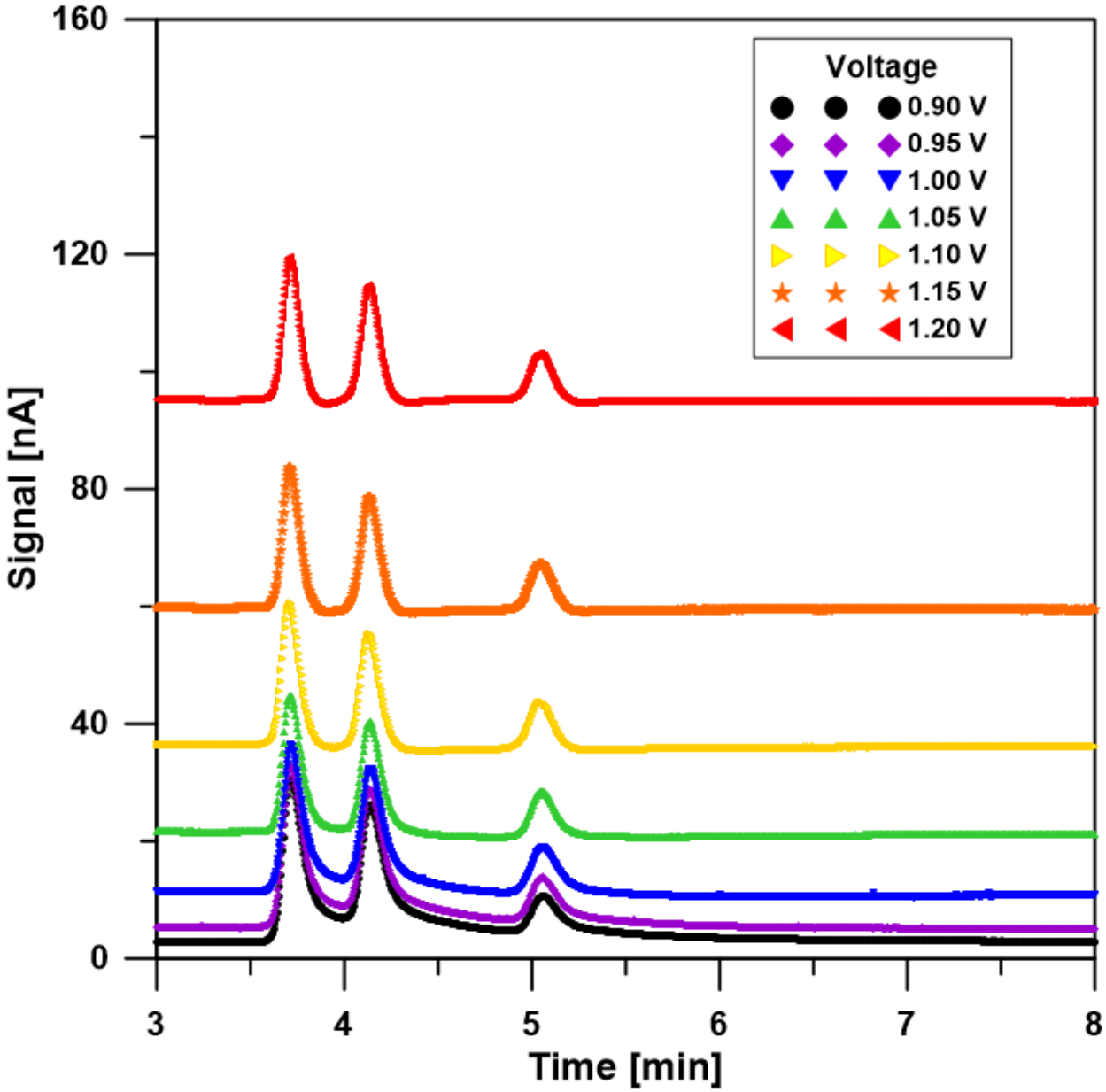

Figure 11. Unscaled chromatograms as operating potential was increased linearly, to help reflect shifts in background as well as peak shape effects. Isocratic injections of a mixture of glucose, fructose, and sucrose, 100 ppm each. Operating potentials are changed from 0.900 V to 1.200 V, every 0.050 V. Other conditions same as in Figure 7.

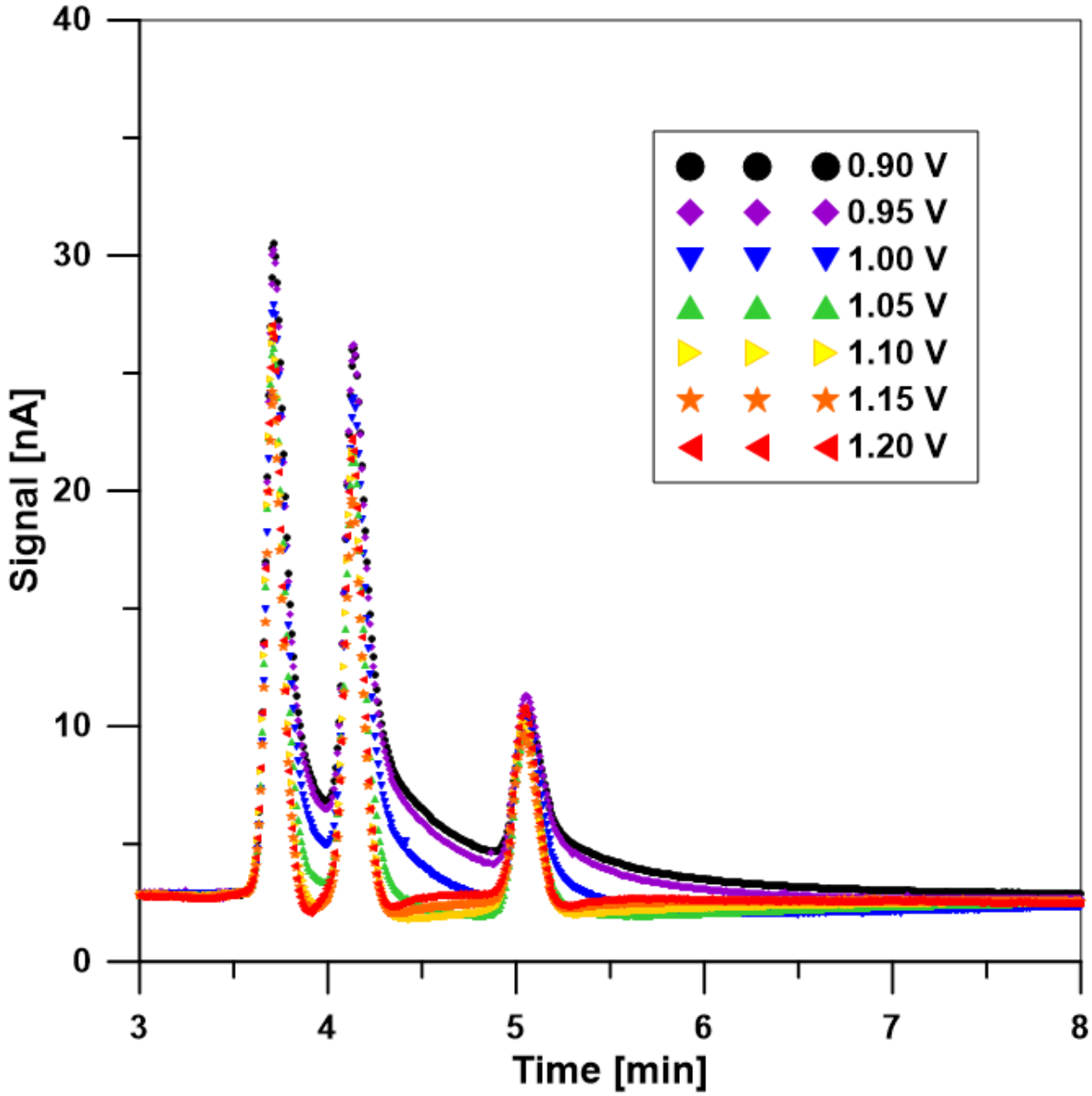

Figure 12. Chromatograms at different applied potentials. The starting baseline was adjusted to the same value. Injections of a mixture of glucose, fructose, and sucrose, 100 ppm each. Operating potentials are changed from 0.900 V to 1.200 V in 0.050 V steps. Other conditions same as in Figure 7.

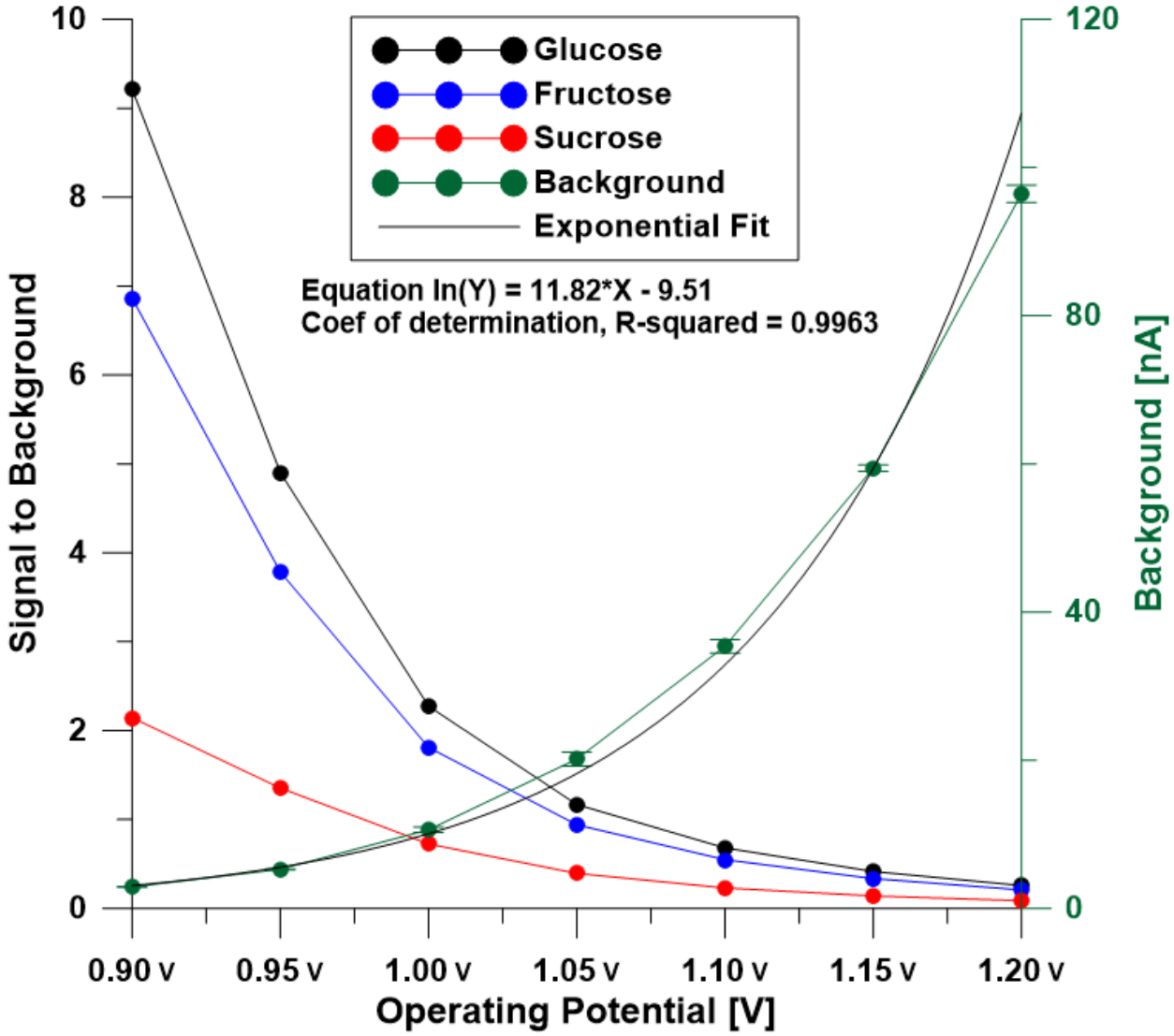

Figure 13. Signal-to-background of glucose, fructose, and sucrose. Isocratic injections of a mixture of glucose, fructose, and sucrose, 100 ppm each. Operating potentials are changed from 0.900 V to 1.200 V, every 0.050 V. Other conditions same as in Figure 7.

Prima facie this would suggest that a lower applied potential would be preferred for a lower LOD. However, pronounced chromatographic tailing as observed in Figures 11 and 12 would dictate that a higher applied potential should be selected for chromatographic analysis to get better peak resolution. However, it does not seem that there are significant improvements in peak tailing beyond an applied potential of 1.10 V while the SNR will continue to decrease. An applied voltage beyond 1.10 V is thus unwarranted.

Change in Retention Factor as a Function of Hydroxide Eluent Concentration. Other important parameters such as retention time and the resolution between peaks on the other hand depends primarily upon the eluent concentration. Since carbohydrates are very weak acids that must be deprotonated to be retained on an anion exchange column, the pH which is dependent on the hydroxide eluent concentration becomes critically important. Increasing KOH concentration reduces retention for the carbohydrates as seen in Figure 14. According to theory, there are several parameters which affect the retention time of the analyte, or selectivity of a certain anion.[54] Parameters that affect the selectivity coefficient include size, charge magnitude (sometimes called electroselectivity), degree of hydration, and polarizability of the eluent and the analyte ions.[54] Here the only parameter that might be changing with eluent concentration is degree of ionization, it is unlikely that the dianion is formed but the degree of ionization certainly changes with increasing pH, The pK_a values of glucose, fructose, and sucrose are respectively, 12.28, 12.03, and 12.62.[53] It will be observed that depending on the eluent concentration, sucrose can be made to elute before, after,

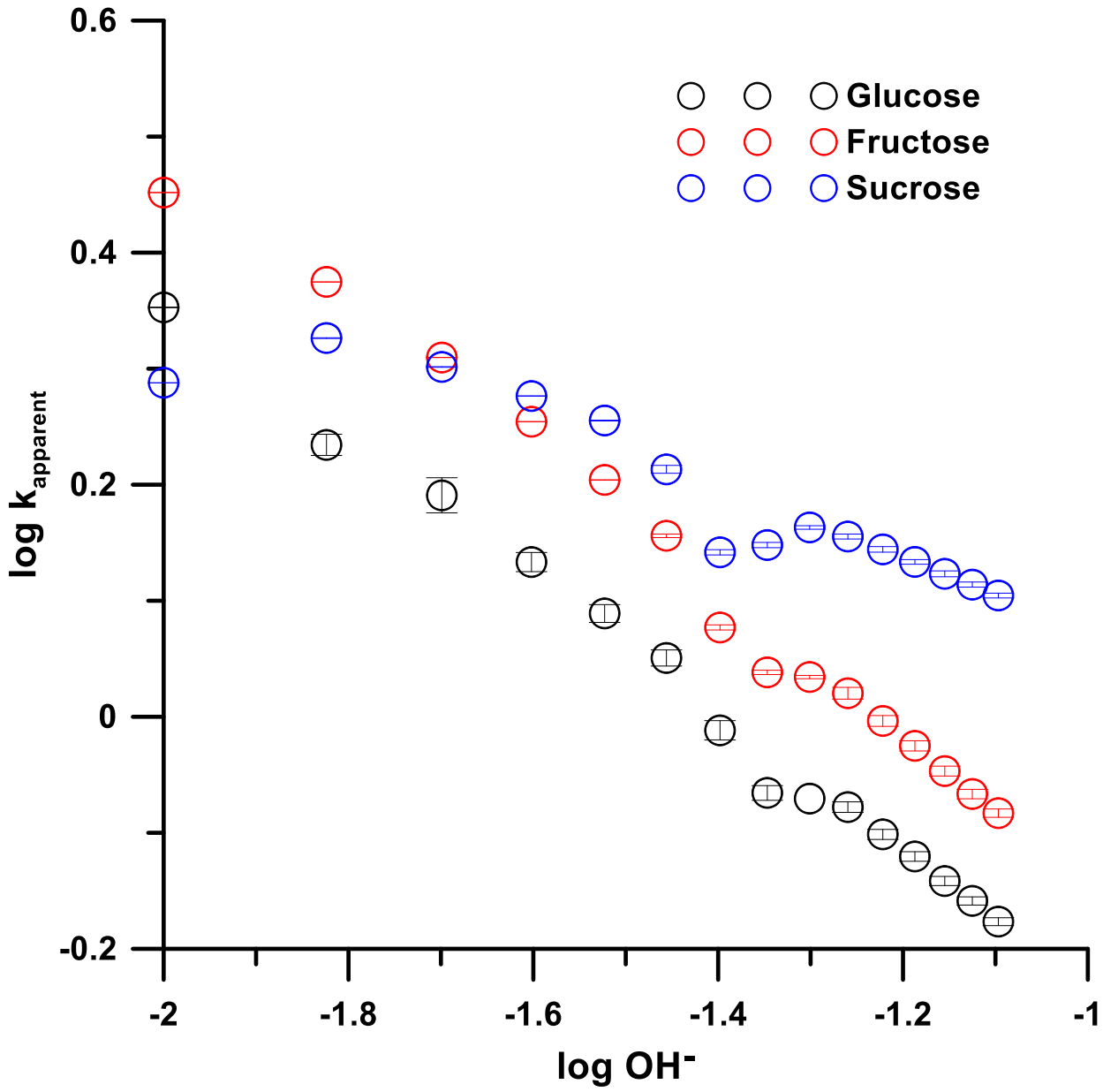

Figure 14. KOH concentration-retention time relationship. Illustrating shift of retention as KOH concentration is increased from 10 mM KOH to 80 mM KOH. Column: 1 mm x 250 mm Dionex CarboPAC PA200 column, particle size: 5, functional group: Quaternary Ammonium Functionalized Latex. Analyte Concentration: 100 ppm each. Flow Rate: 50 µL/min. Injection Volume: 400 nL. Eluent Concentration: 10-80 mM KOH. Column Temperature: 30 °C. Electrochemical Detector settings: voltage, 0.940 V; data collection frequency, 20 Hz; rise time, 0.50 s. Pneumatic Pressure on Piston: 5 psi

or in between fructose and glucose (the sucrose k values cross those of glucose and fructose). In Figure 14, we designate the observed k values as $k_{apparent}$ as none of the analytes are fully ionized; in the following the true k values of the corresponding anions are referred to as k_{true}. If the neutral sugar is not retained, it will be apparent that the relationship between k_{true} and $k_{apparent}$ will be given as:

$$k_{apparent} = \alpha * k_{true} \quad \ldots(2)$$

or

$$k_{true} = k_{apparent}/\alpha \quad \ldots(3)$$

where α, the degree of dissociation of each individual sugar, is given by

$$\alpha = K_a/(K_a + [H^+]) \quad \ldots(4)$$

Strictly, all terms in eq 4 should be in terms of concentration. The activity coefficients of H^+ and OH^- in a KOH eluent in the concentration range studied is easily computed; however, K_a in concentration terms is not easily computed because of the difficulty in estimating the size of the sugar anion. In addition, treating, e.g., α-D-glucose as an acid with a single ionizable proton may not be appropriate: computational algorithms, e.g.chemicalize.com provides the pK_a for the 5 hydroxylic protons for dextrose to range from 11.30 to 15.12. Likely at least the two most acidic protons (pK_a 11.30 and 12.69) will contribute, and the corresponding monoanions may not have the same retention. Here the simple treatment of considering the glucose and the other sugars as simple monoprotic acids with pK_a values as previously stated, without any activity correction is adopted. The computed fractional dissociation values for the three analytes at the different eluent concentrations are shown in Figure 15.

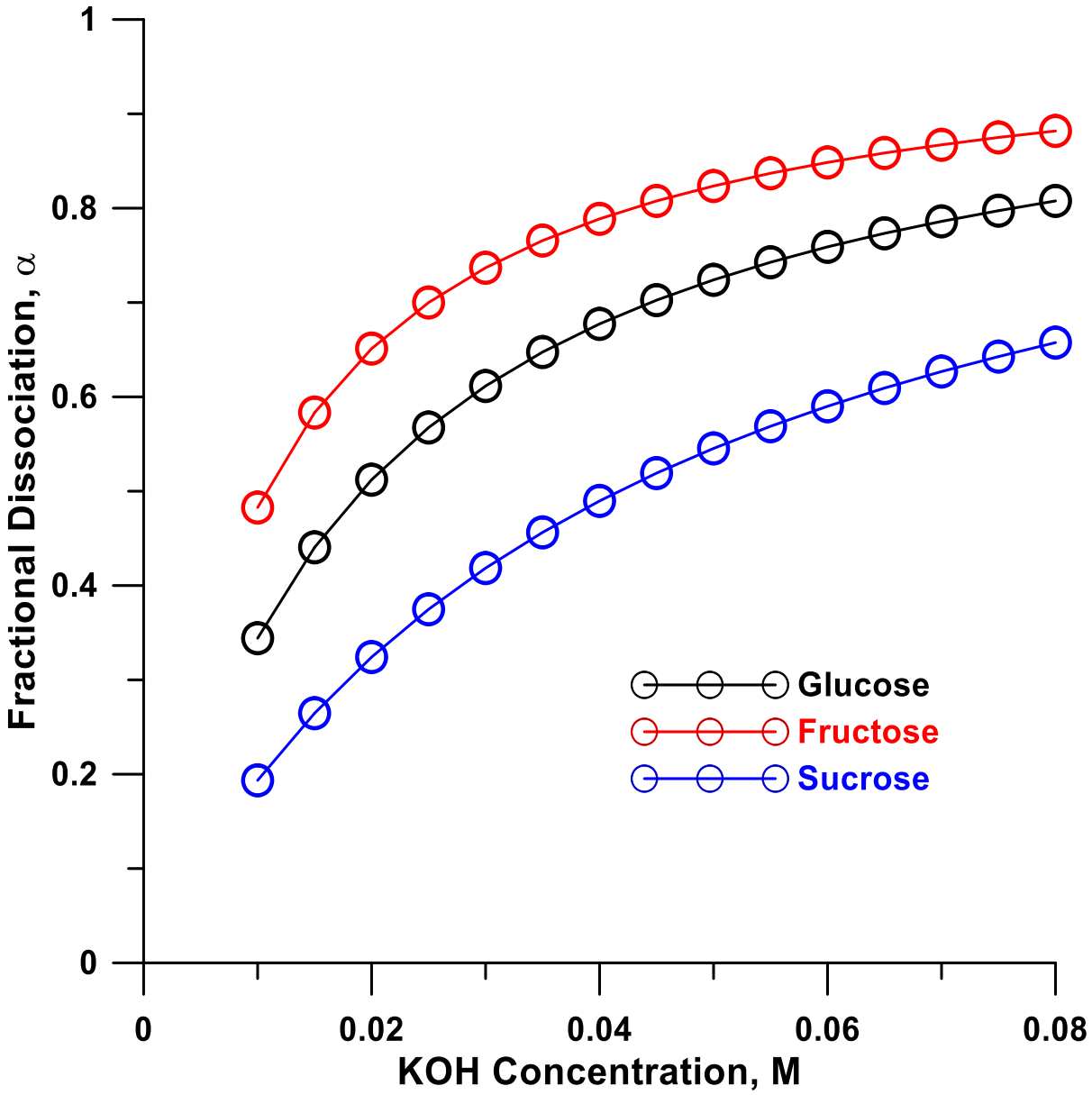

Figure 15. Fractional dissociation α as a function of eluent KOH concentration, computed according to eq 4.

For simple fully dissociated ions, it is well known in IC that plots of the log of the retention factor, k, and the of the eluent concentration yield a straight line whose slope is equal to the ratio of the charge between the analyte and eluent ion.[54] However, consideration of Figure 14 does not indicate a generally linear monotonically increasing relationship; indeed, for sucrose the retention actually increases from 10 to 15 mM KOH as eluent.

As the sugars themselves are by nature weak acids, increasing eluent concentration in the range studied (10-80 mM KOH), that corresponds to a nominal pH range (without activity correction) of 12 to 12.9, all of the sugars will be partially ionized in this range (nominally 34-81% for glucose, 48-88% for fructose, and 19-66% for sucrose; the degree of ionization is depicted in Figure 15), there are then two conflicting forces that drive the retention of these ions. If we assume that only the ionized form of the sugar is retained by the stationary phase, increasing hydroxide eluent concentration will reduce retention while increasing ionization will promote retention. Instead of plotting log $k_{apparent}$ vs. log [OH^-] we can combine the data in Figures 14 and 15 to compute k_{true} according to eq 3, then plot the resulting log k_{true} vs. log [OH^-] in Figure 16. Although such a plot is still not strictly linear (r^2 ranges from 0.9824 to 0.9900) it is far more linear than before. It is also now strictly a monotonic change - there is no increase in the log k value for sucrose from 10 mM to 15 mM KOH eluent.

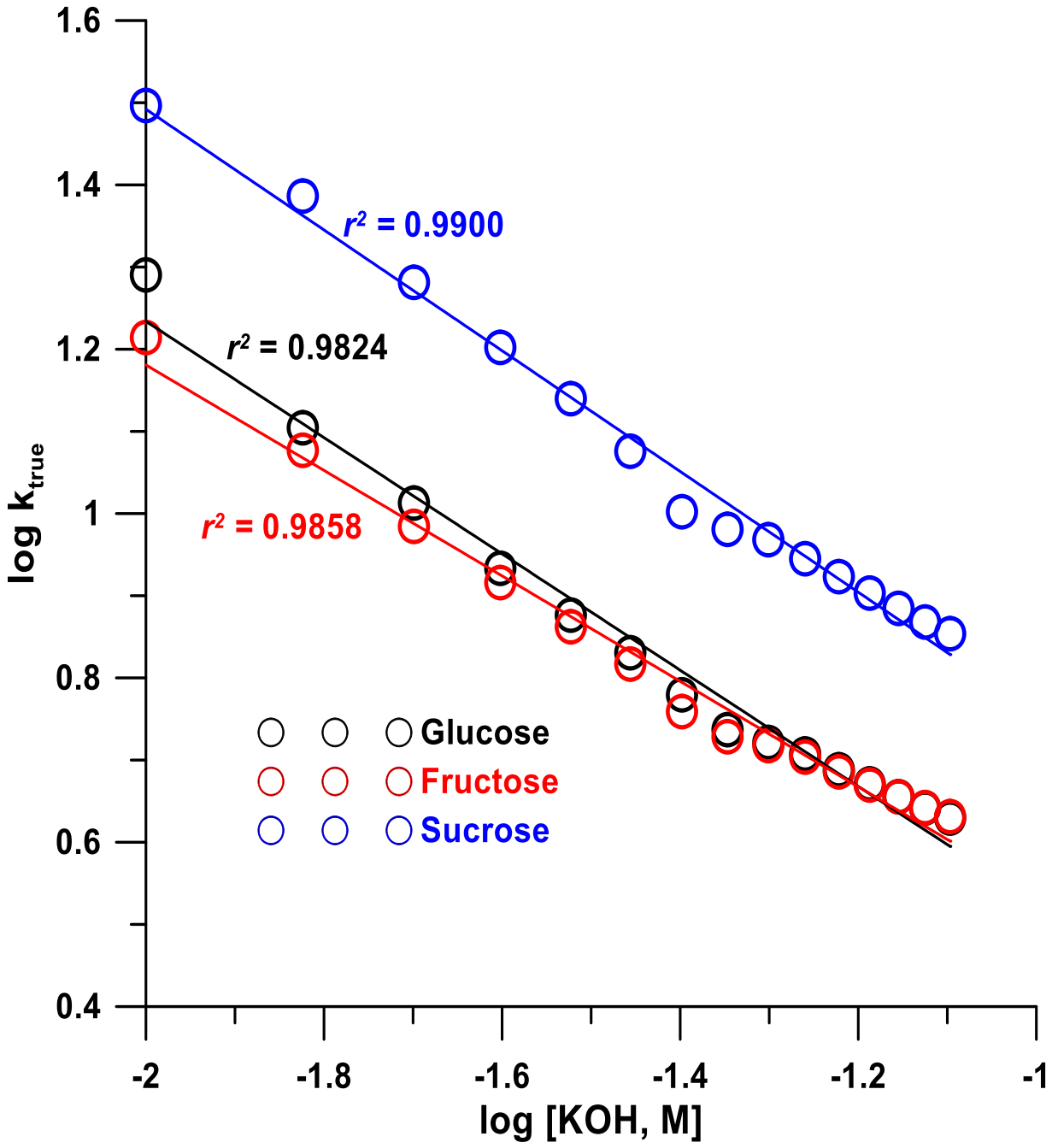

Figure 16. log k_{true} vs. log eluent concentration.

It is interesting to note, however, that the data in Figure 16 may be better interpreted in a different manner. With the possible exception of the lowest eluent concentration data the rest of the data for each analyte fall in two distinct linear groups, as shown in Figure 17. It will be noted that in all cases the slope of the line at higher eluent concentrations is lower than that at lower eluent concentrations, as would be expected if a more charged analyte anionic entity is formed at higher eluent concentrations. In neither region, however, an integer slope is observed. The relevant data for sucrose is indicated in the figure, these slopes will indicate that in both regions the anion is carrying a charge less than 1. If a different species is being formed at higher pH, it could be effectively less retained than the anion that is present at a lower pH. Similar results are seen for glucose and fructose. A detailed understanding of this behavior is presently lacking. However, treating the sugars as simple monoprotic acids are likely inappropriate. Computational predictions for glucose, for example from Chemicalize.com predict the pK_a's depicted in Figure 18.

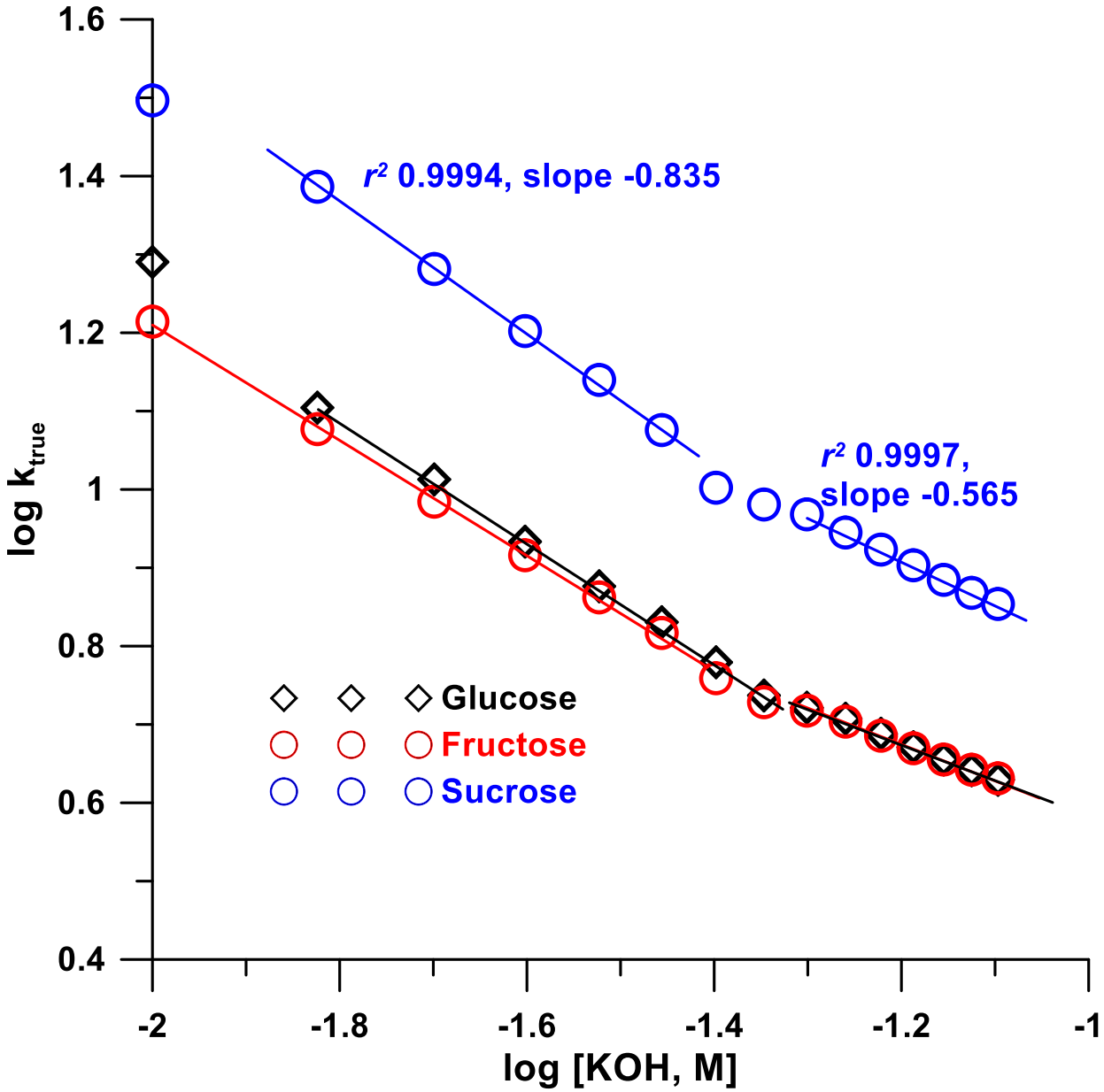

Figure 17. The data in Figure 16 may be better interpreted with two separate linear regions. See text for details.

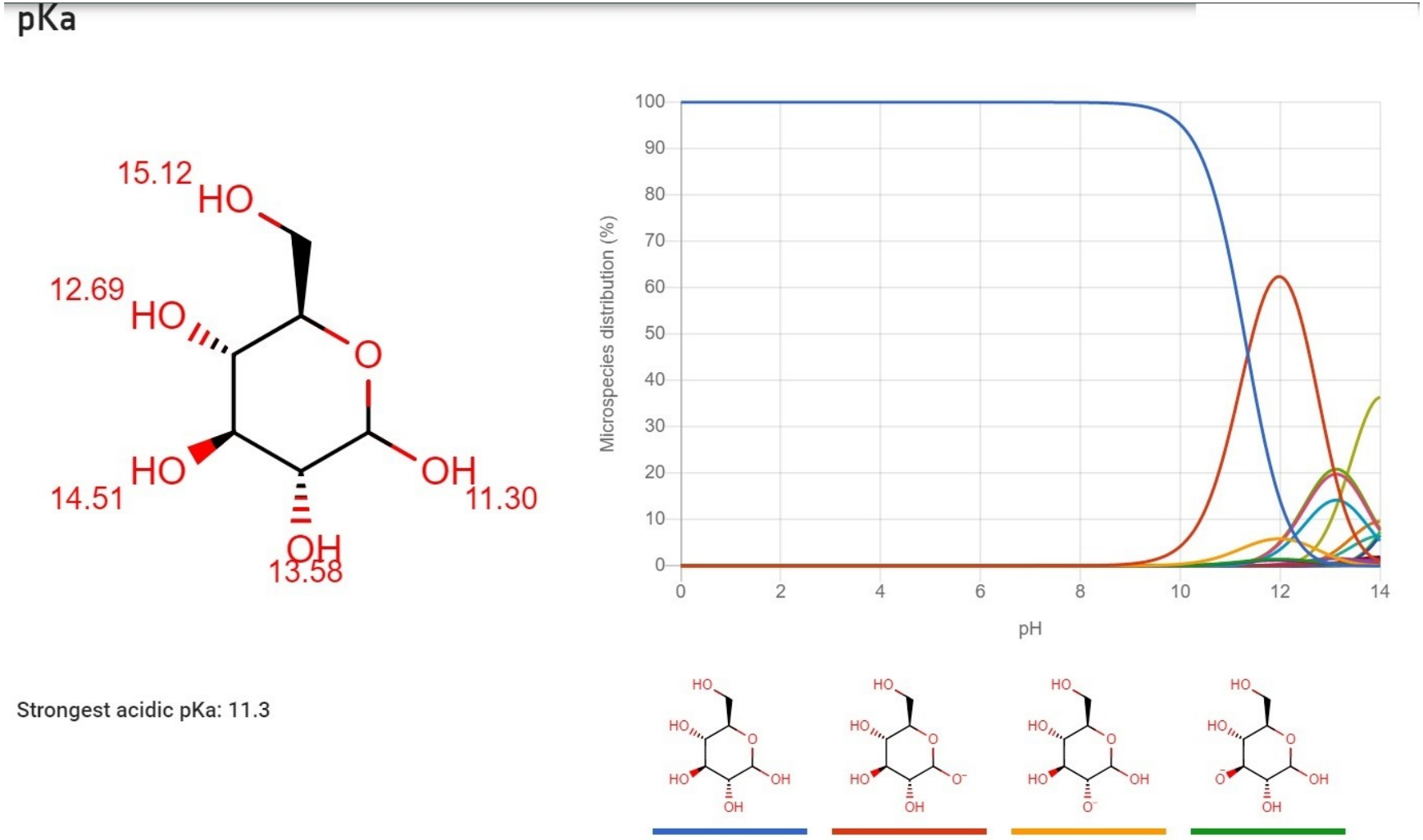

Figure 18. Micro acid dissociation constants for the different hydroxylic protons of glucose. This output was generated by freely accessible web computational service at Chemicalize.com

It will be noted that the most acidic micro pK_a of glucose (11.30) is significantly more acidic compared to the nominal pKa of glucose (12.28). A monoanion may also form *instead* through the ionization of the second most acidic proton (pK_a 12.69). However, the ratios of these two monoanion species will remain constant regardless of pH and even if the retention factors of the two separate monoanions are different. Therefore, the effective weighted retention factor will still behave the same as in the case of a simple monoanion and cannot explain the observed behavior. However, in a pH range that spans up to 12.9, significant amounts of the dianion where both the first and the second proton is lost, can be formed (Figure 19). In this case, the dianion to monoanion ratio will not remain constant with pH, as seen in Figure 19. Normally a dianion is more retained than the monoanion but there can be exceptions due to steric reasons. If one site is interacting with the stationary phase, the second site may be sterically positioned such that it becomes impossible for it to interact simultaneously with the stationary phase. Mo[55] has observed that while naphthalenedisulfonate is more strongly retained in an open tubular anion exchange column than naphthalenemonosulfonate, The trisulfonate elutes in between the two, as it is sterically impossible for the third sulfonate group to simultaneously interact with the anion exchange sites. The hydrophilic ionized group interacting with the solvent reduces retention. Similar behavior has been reported for the *myo*-inositol phosphates: while the diphosphates elute after the monophosphate, the triphosphates elute before most of the diphosphates, the hexaphosphates elute before either the tetra or pentaphosphates and several of the pentaphosphates elute before several of the tetraphosphates.[56]

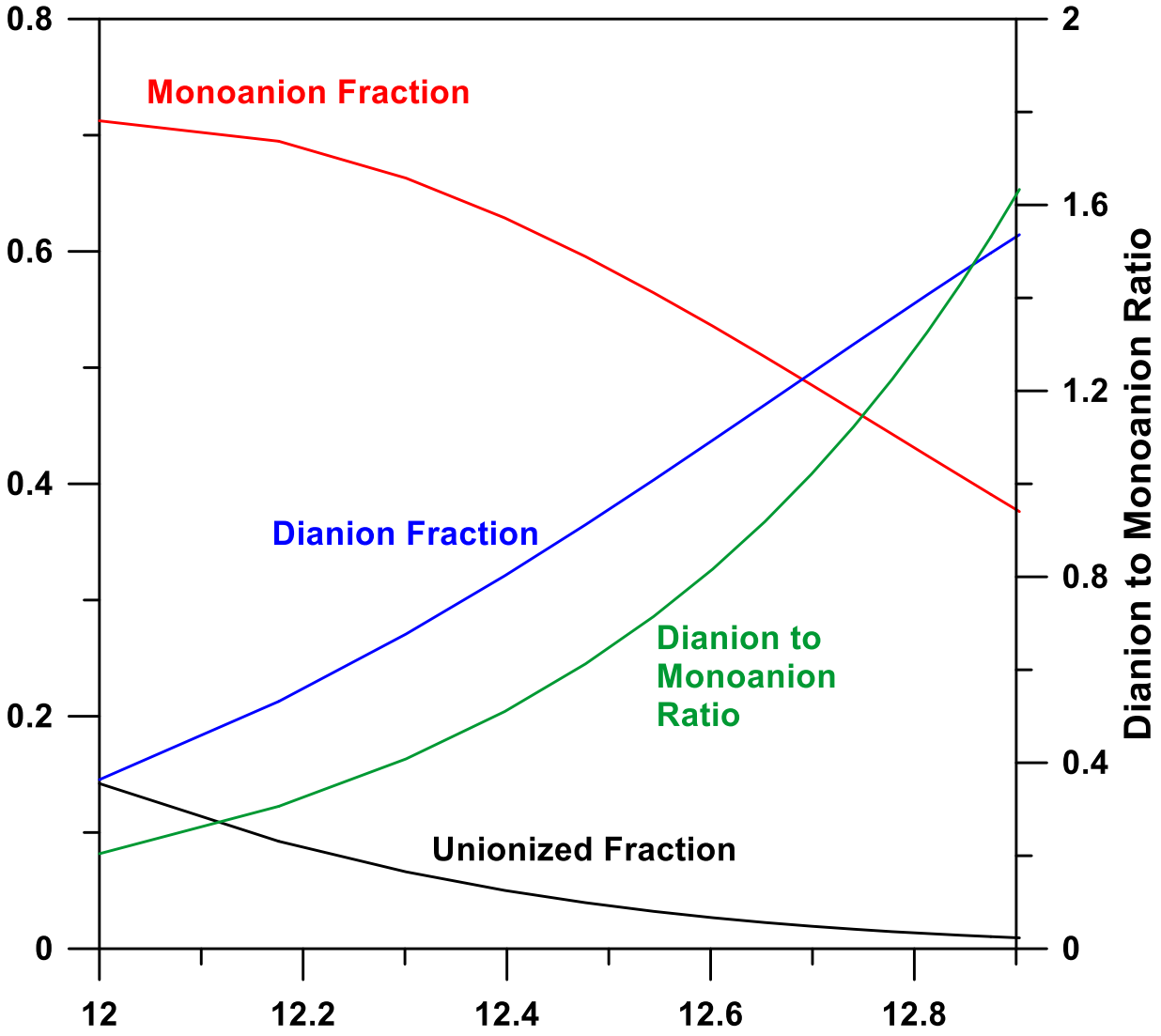

Figure 19. Distribution of unionized glucose and the mono- and dianion and the dianion/monoanion ratio computed using the microdissociation constants listed in Figure 18.

Separation of Glucose, Fructose and Sucrose.

Above 30 mM KOH, all three peaks were baseline resolved from one another. However, at eluent concentrations greater than 70 mM KOH, glucose and fructose could no longer be baseline resolved. To minimize the separation time but still maintain good resolution, 60 mM KOH was selected as eluent to carry out further experiments to study reproducibility.

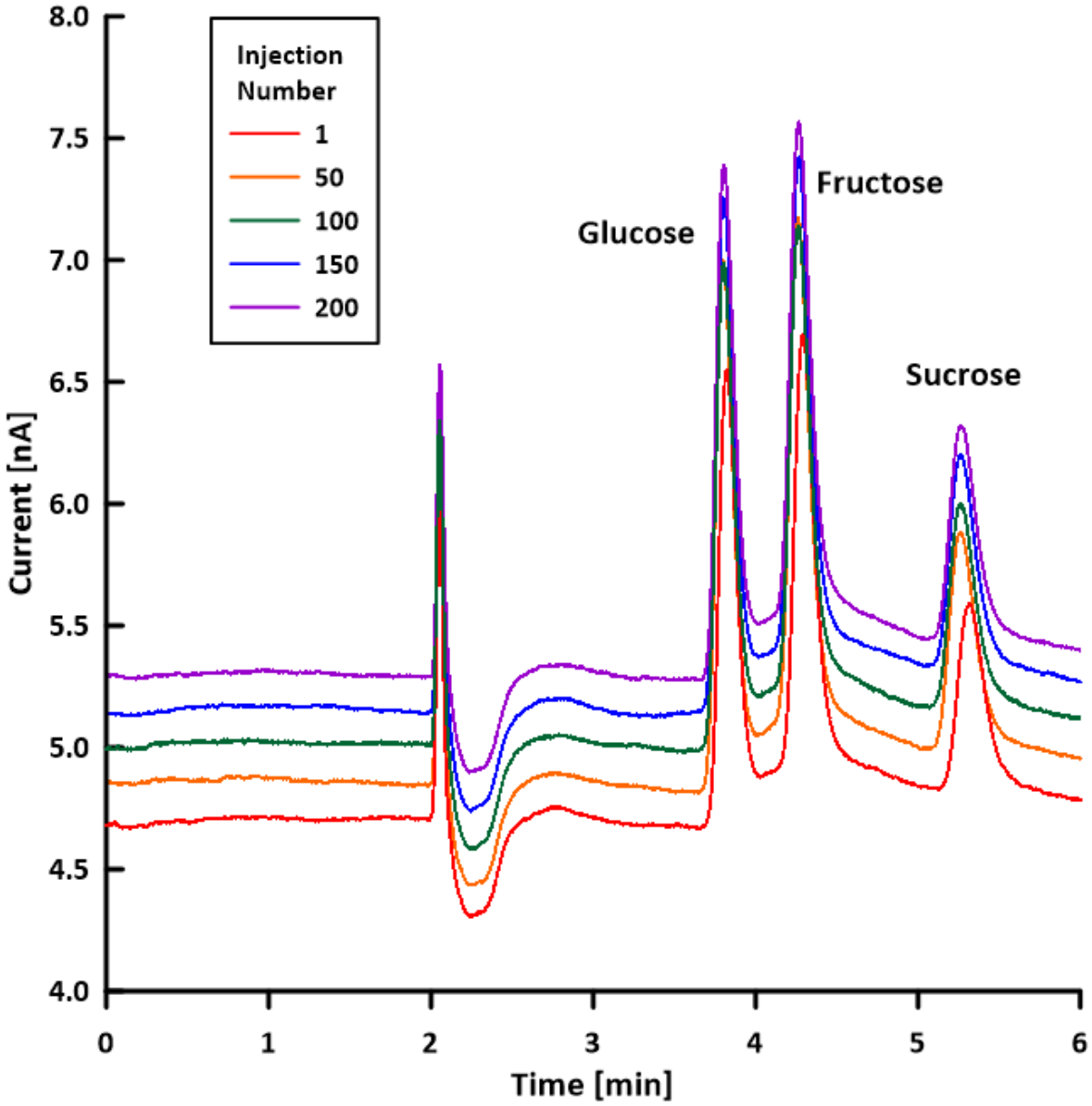

Figure 20. Reproducibility of HPAE separation of glucose, fructose, and sucrose with detection by DC amperometry on a self-positioning copper electrode. Beginning with the first injection, the data shown are for every 50th injection up to 200 injections. The retention time for glucose, fructose, and sucrose were 3.80, 4.26, and 5.26 min, respectively. 60 mM KOH eluent. Other conditions same as in Figure 14.

Performance and Reproducibility of the HPAE- Self-positioning Copper Electrode DC Amperometry System.

Over 200 injections were carried out with the system (Figures 20 and 21) to observe reproducibility. The parameters studied include peak width, retention time and peak height to observe and the reproducibility over continuous analysis. Figure 20 illustrates five different chromatograms at injection number 1, 50, 100, 150, and 200; each chromatogram shown is roughly 6 hours apart. The overlaid chromatograms facilitate an evaluation of the reproducibilities of the retention time and the detector response involved over a period of continuous analysis for exceeding 24 hours. This performance is in remarkable contrast to the DC amperometry performance of the gold electrode as shown in Figure 4, where the response decreases continuously. It is to be noted that the superior performance of the present system is owed both to the consumption of the copper electrode, regenerating a fresh surface *and* the automatic repositioning of the electrode. These results suggest that the present arrangement is well-suited for the separation and detection of simple carbohydrates and perhaps other analytes.

In Figure 20, it may be observed that the first injection (red trace) exhibits a slightly longer retention time – the same is also more readily noted in Figure 21 (black trace). It is likely that the system was not fully equilibrated when the experiment started. The traces in Figure 21 show no indications of changing efficiency or peak shape over time. However, the baseline did shift over time. This is shown in Figure 22, However, as Figure 22 also shows, peak response did not show a similar systematic change over time. An increased in area of the electrode face is known to increase both baseline current and peak height, noise also increases.[44] The fact that the height or area

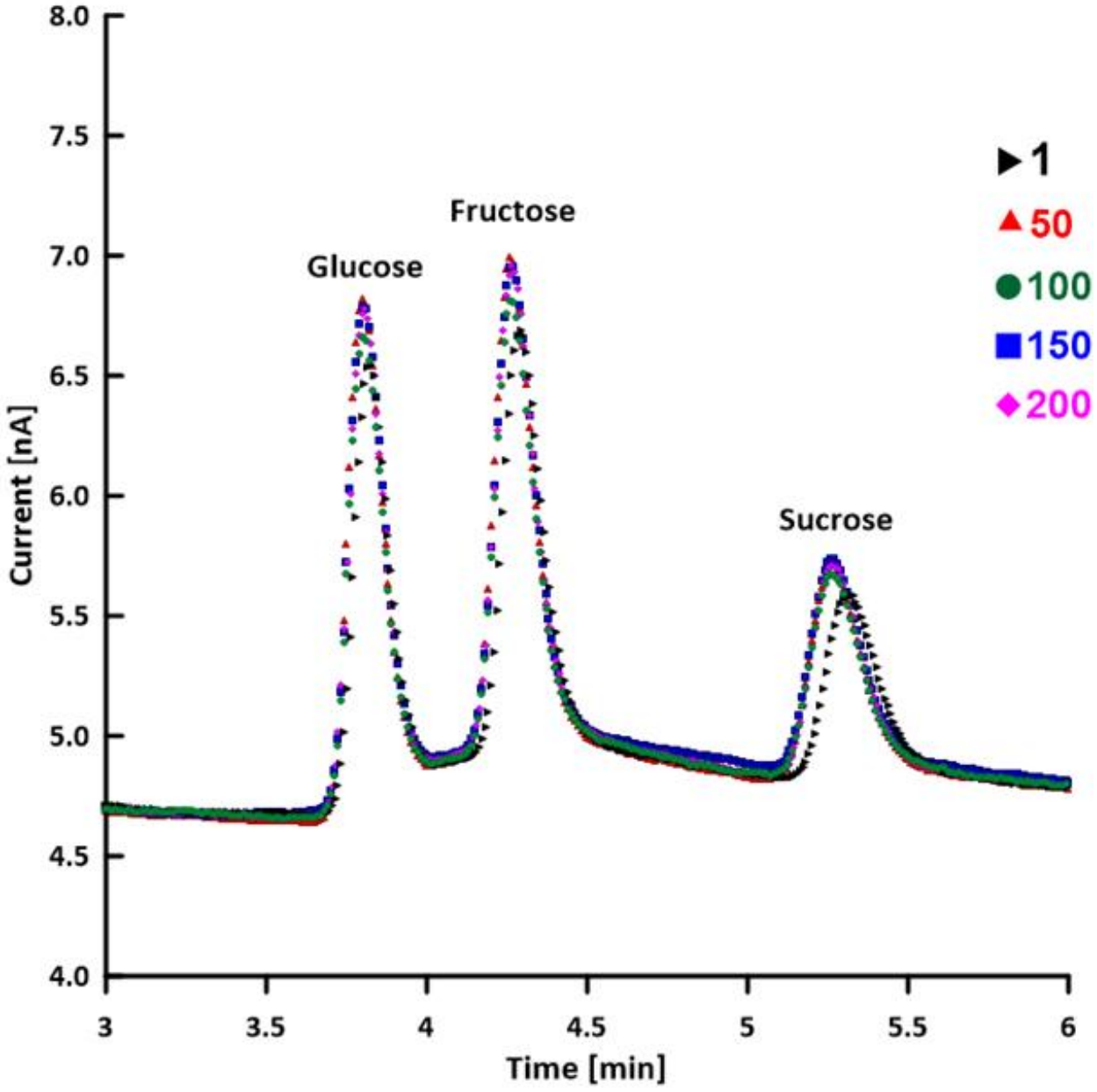

Figure 21. Chromatograms are adjusted to the same starting baseline. Every 50th chromatogram is shown to illustrate reproducibility over an extended period of time. Conditions same as in Figure 20.

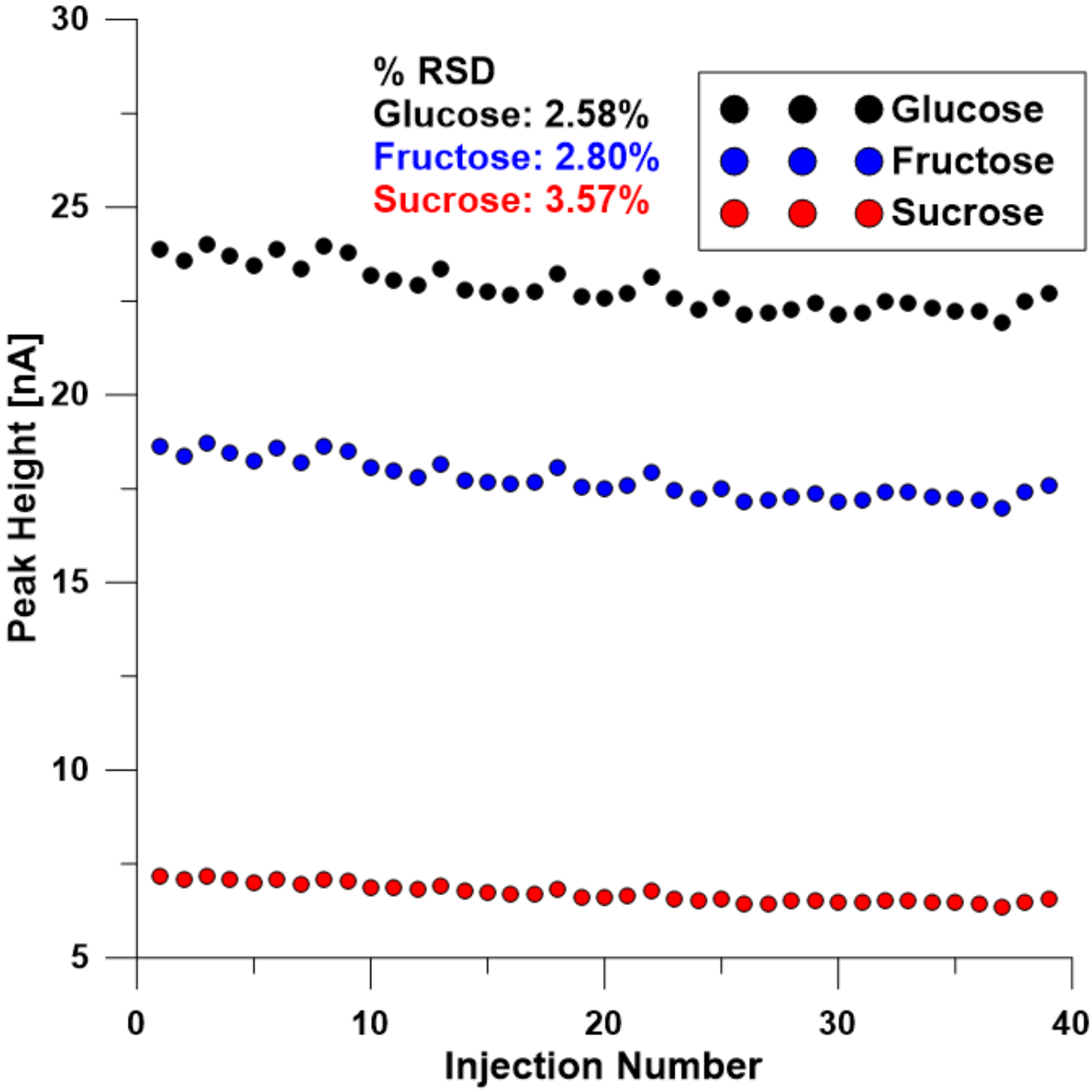

Figure 22. Peak height vs. injection number. Isocratic injections of a mixture of glucose, fructose, and sucrose, 100 ppm each. Operating potentials are changed from 0.900 V to 1.200 V, every 0.050 V. Other conditions the same as in Figure 7.

response (Figure 23) does not increase over time suggests that a change in electrode diameter, leading to an increase in exposed surface area, is not the reason for the increase in the background current.

Noise Performance and Response Reproducibility. The rms noise of the system was calculated over a 20 s wide interval, approximately equal to the width of the widest peak, that due to sucrose (19 ± 2 seconds). Over 40 injections, the rms noise of the baseline was found to be 54 ± 4 pA.

Peak area or peak heights are often used for specifying quantitative reproducibility of a measurement. Peak heights and areas of 40 injections are shown for each analyte in Figures 22 and 23, respectively. The cell was maintained at a temperature-controlled enclosure at 35 °C. There was no observable signal decay; the variability in data ranged from 2.38-2.94 % and 2.58-3.57 % for peak height and area, respectively, signals were well correlated (R^2 = 0.99).

Response fluctuations are random between injections and appear to affect each analyte in a similar manner. This could be compensated for by incorporation of an internal standard. It is possible that this is due to minute changes is interelectrode distance as the pressurized system moves the electrode. If this is true, a further increase in pressure behind the electrode may be beneficial. A systematic study on the pressure behind the electrode as well as exit restriction on the cell is warranted.

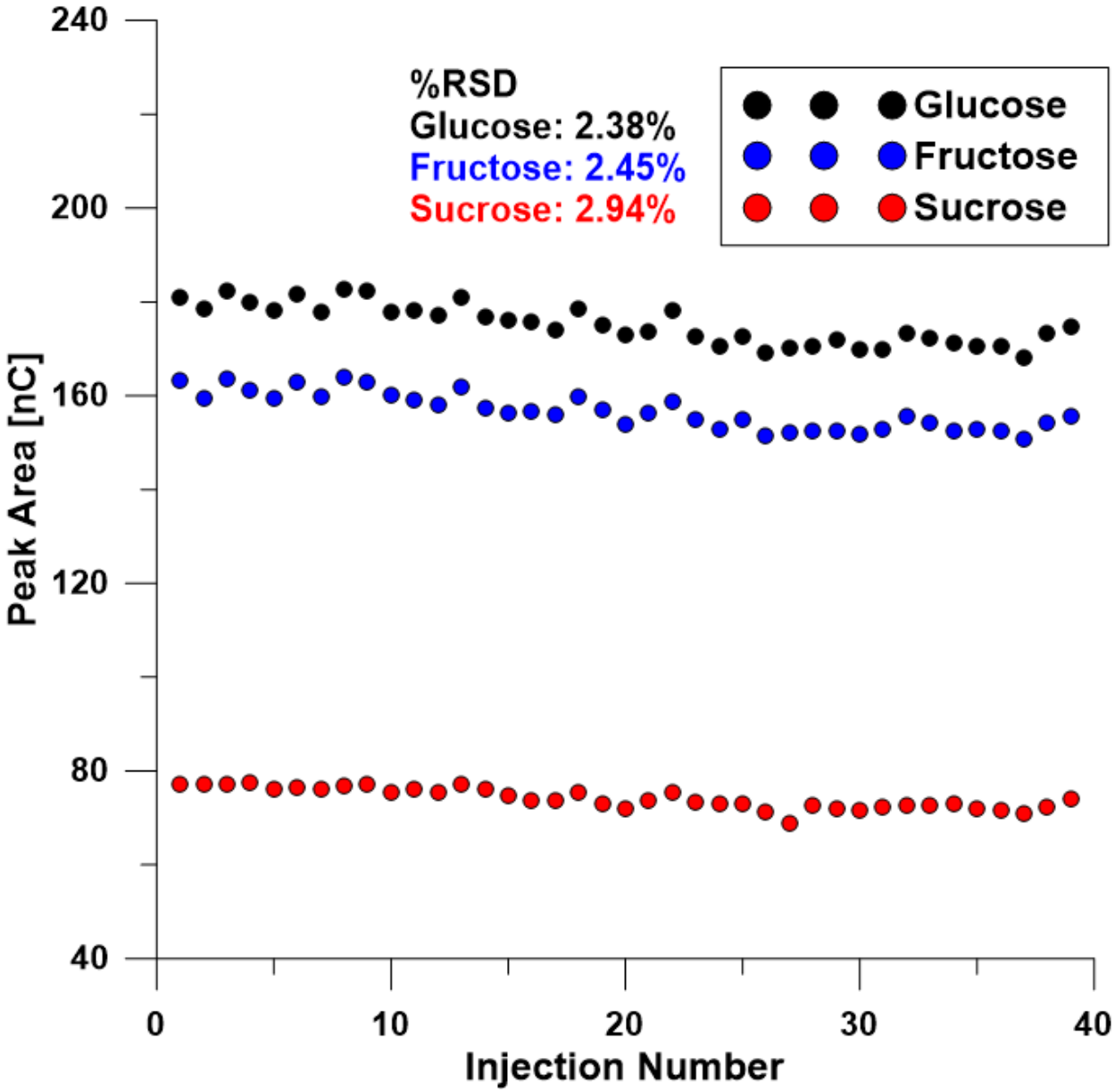

Figure 23. Peak area vs. injection number. Isocratic injections of a mixture of glucose, fructose, and sucrose, 100 ppm each. Operating potentials are changed from 0.900 V to 1.200 V, every 0.050 V. Other conditions same as in Figure 7.

Chapter 4

Conclusions

This work shows the feasibility of an automated arrangement that maintains an electrode that is consumed in the detection process, at a constant distance from the counter electrode. Specific embodiment using a copper wire electrode in the constant potential amperometric detection mode for the detection of carbohydrates was demonstrated. Further research is ongoing to demonstrate compatibility with gradient elution and separation and detection of carbohydrate oligomers. Such a demonstration will indicate the potential utility of the approach for the analysis of glycans, steroids, starches, glycogens, and more, of great importance to the food and pharmaceutical industries.

References

(1) McClements, D. J. *Food Emulsions: Principles, Practices, and Techniques* | *D. J. McClements* | *Download*, 2nd ed.; CRC Press, 2005.

(2) Li, M.; Du, J.; Zhang, K. Profiling of Carbohydrates in Commercial Beers and Their Influence on Beer Quality. *J. Sci. Food Agric.* **2020**, *100* (7), 3062–3070. https://doi.org/10.1002/jsfa.10337.

(3) Chen, Y.; Barreto, V.; Woodruff, A.; Lu, Z.; Liu, Y.; Pohl, C. Dual Electrolytic Eluent Generation for Oligosaccharides Analysis Using High-Performance Anion-Exchange Chromatography. *Anal. Chem.* **2018**, *90* (18), 10910–10916. https://doi.org/10.1021/acs.analchem.8b02436.

(4) James, C. S. *Analytical Chemistry of Foods*, 1st ed.; 1995.

(5) Appelmelk, B. J.; van Die, I.; van Vliet, S. J.; Vandenbroucke-Grauls, C. M. J. E.; Geijtenbeek, T. B. H.; van Kooyk, Y. Cutting Edge: Carbohydrate Profiling Identifies New Pathogens That Interact with Dendritic Cell-Specific ICAM-3-Grabbing Nonintegrin on Dendritic Cells. *J. Immunol.* **2003**, *170* (4), 1635–1639. https://doi.org/10.4049/jimmunol.170.4.1635.

(6) Jayasena, V.; Cameron, I. °brix/Acid Ratio as a Predictor of Consumer Acceptability of Crimson Seedless Table Grapes. *J. Food Qual.* **2008**, *31* (6), 736–750. https://doi.org/10.1111/j.1745-4557.2008.00231.x.

(7) Kupina, S.; Roman, M. Determination of Total Carbohydrates in Wine and Wine-like Beverages by HPLC with a Refractive Index Detector: First Action 2013.12. *J. AOAC Int.* **2014**, *97* (2), 498–505. https://doi.org/10.5740/jaoacint.13-320.

(8) Damayanti, S.; Permana, B.; Weng, C. Determination of Sugar Content in Fruit

Juices Using High Performance Liquid Chromatography. *Acta Pharm. Indones.* **2012**, *37* (4), 131–139.

(9) Schenk, J.; Nagy, G.; Pohl, N. L. B.; Leghissa, A.; Smuts, J.; Schug, K. A. Identification and Deconvolution of Carbohydrates with Gas Chromatography-Vacuum Ultraviolet Spectroscopy. *J. Chromatogr. A* **2017**, *1513*, 210–221. https://doi.org/10.1016/j.chroma.2017.07.052.

(10) Aich, U.; Liu, A.; Lakbub, J.; Mozdzanowski, J.; Byrne, M.; Shah, N.; Galosy, S.; Patel, P.; Bam, N. An Integrated Solution-Based Rapid Sample Preparation Procedure for the Analysis of N-Glycans from Therapeutic Monoclonal Antibodies. *J. Pharm. Sci.* **2016**, *105* (3), 1221–1232. https://doi.org/10.1016/j.xphs.2015.12.022.

(11) Stacey, M.; Nashabeh, W. Carbohydrate Analysis of a Chimeric Recombinant Monoclonal Antibody by Capillary Electrophoresis with Laser-Induced Fluorescence Detection. *Anal. Chem.* **1999**, *71* (22), 5185–5192. https://doi.org/10.1021/ac990376z.

(12) Volpi, N. *Capillary Electrophoresis of Carbohydrates*, 1st ed.; Volpi, N., Ed.; Humana Press, 2011. https://doi.org/https://doi.org/10.1007/978-1-60761-875-1.

(13) Gao, X.; Yang, J.; Huang, F.; Wu, X.; Li, L.; Sun, C. Progresses of Derivatization Techniques for Analyses of Carbohydrates. *Anal. Lett.* **2003**, *36* (7), 1281–1310. https://doi.org/10.1081/AL-120021087.

(14) Huang, Y.; Mechref, Y.; Novotny, M. V. Microscale Nonreductive Release of O-Linked Glycans for Subsequent Analysis through MALDI Mass Spectrometry and Capillary Electrophoresis. *Anal. Chem.* **2001**, *73* (24), 6063–6069.

https://doi.org/10.1021/ac015534c.

(15) Bottcher, J.; Margraf, M.; Monks, K. *Liquid Chromatography | HPLC Systems | KNAUER*; Berlin.

(16) Joseph, M. *No Title*.

(17) Vehovec, T.; Obreza, A. Review of Operating Principle and Applications of the Charged Aerosol Detector. *Journal of Chromatography A*. Elsevier March 5, 2010, pp 1549–1556. https://doi.org/10.1016/j.chroma.2010.01.007.

(18) Rohrer, J. S.; Kitamura, S. Determination of Carbohydrates Using Liquid Chromatography with Charged Aerosol Detection. In *Charged Aerosol Detection for Liquid Chromatography and Related Separation Techniques*; Gamache, P. H., Ed.; John Wiley & Sons, Inc.: Hoboken, NJ, USA, 2017; pp 311–325. https://doi.org/10.1002/9781119390725.ch7.

(19) Almeling, S.; Ilko, D.; Holzgrabe, U. Charged Aerosol Detection in Pharmaceutical Analysis. *Journal of Pharmaceutical and Biomedical Analysis*. Elsevier October 1, 2012, pp 50–63. https://doi.org/10.1016/j.jpba.2012.03.019.

(20) Leijdekkers, M. Characterization of Sugar Beet Pulp Derived Oligosaccharides, Wageningen University, 2015.

(21) Szabo, Z.; Guttman, A.; Rejtar, T.; Karger, B. L. Improved Sample Preparation Method for Glycan Analysis of Glycoproteins by CE-LIF and CE-MS. *Electrophoresis* **2010**, *31* (8), 1389–1395. https://doi.org/10.1002/elps.201000037.

(22) Zygler, A.; Wasik, A.; Kot-Wasik, A.; Namieśnik, J. Determination of Nine High-Intensity Sweeteners in Various Foods by High-Performance Liquid Chromatography with Mass Spectrometric Detection. *Anal. Bioanal. Chem.* **2011**,

400 (7), 2159. https://doi.org/10.1007/S00216-011-4937-Z.

(23) Reusch, D.; Haberger, M.; Maier, B.; Maier, M.; Kloseck, R.; Zimmermann, B.; Hook, M.; Szabo, Z.; Tep, S.; Wegstein, J.; Alt, N.; Bulau, P.; Wuhrer, M. Comparison of Methods for the Analysis of Therapeutic Immunoglobulin G Fc-Glycosylation Profiles—Part 1: Separation-Based Methods. *MAbs* **2015**, *7* (1), 167–179. https://doi.org/10.4161/19420862.2014.986000.

(24) Rohrer, J. S.; Basumallick, L.; Hurum, D. C. Profiling N-Linked Oligosaccharides from IgG by High-Performance Anion-Exchange Chromatography with Pulsed Amperometric Detection. *Glycobiology* **2016**, *26* (6), 582–591. https://doi.org/10.1093/glycob/cww006.

(25) Davies, M. J.; Hounsell, E. F. Carbohydrate Chromatography: Towards Yoctomole Sensitivity. *Biomed. Chromatogr.* **1996**, *10* (6), 285–289. https://doi.org/10.1002/(SICI)1099-0801(199611)10:6<285::AID-BMC616>3.0.CO;2-W.

(26) Rocklin, R. D.; Pohl, C. A. Determination Of Carbohydrates By Anion Exchange Chromatography With Pulsed Amperometric Detection. *J. Liq. Chromatogr.* **1983**, *6* (9), 1577–1590. https://doi.org/10.1080/01483918308064876.

(27) Brunt, K. Comparison between the Performances of an Electrochemical Detector Flow Cell in a Potentiometric and an Amperometric Measuring System Using Glucose as a Test Compound. *Analyst* **1982**, *107* (1279), 1261–1271. https://doi.org/10.1039/AN9820701261.

(28) Wang, J.; Cao, X.; Wang, X.; Yang, S.; Wang, R. Electrochemical Oxidation and Determination of Glucose in Alkaline Media Based on Au (111)-like Nanoparticle

Array on Indium Tin Oxide Electrode. *Electrochim. Acta* **2014**, *138*, 174–186. https://doi.org/10.1016/j.electacta.2014.06.116.

(29) Johnson, D. C.; Dobberpuhl, D.; Roberts, R.; Vandeberg, P. Pulsed Amperometric Detection of Carbohydrates, Amines and Sulfur Species in Ion Chromatography - the Current State of Research. *J. Chromatogr. A* **1993**, *640* (1–2), 79–96. https://doi.org/10.1016/0021-9673(93)80171-4.

(30) Johnson, D. C.; LaCourse, W. R. Liquid Chromatography with Pulsed Electrochemical Detection at Gold and Platinum Electrodes. *Anal. Chem.* **1990**, *62* (10), 589A-597A. https://doi.org/10.1021/ac00209a001.

(31) Casella, I. G.; Gatta, M.; Cataldi., T. R. I. Amperometric Determination of Underivatized Amino Acids at a Nickel- Modified Gold Electrode by Anion-Exchange Chromatography. *J. Chromatogr. A* **2000**, *878* (1), 57–67. https://doi.org/10.1016/S0021-9673(00)00274-0.

(32) Neuburger, G. G.; Johnson, D. C. Comparison of the Pulsed Amperometric Detection of Carbohydrates at Gold and Platinum Electrodes for Flow Injection and Liquid Chromatographic Systems. *Anal. Chem.* **1987**, *59* (1), 203–204. https://doi.org/10.1021/ac00128a043.

(33) Noh, M. F. M.; Tothill, I. E. Development and Characterisation of Disposable Gold Electrodes, and Their Use for Lead(II) Analysis. *Anal. Bioanal. Chem.* **2006**, *386* (7–8), 2095–2106. https://doi.org/10.1007/s00216-006-0904-5.

(34) Cheng, J.; Jandik, P.; Avdalovic, N. Disposable Working Electrode for an Electrochemical Cell. 6783645B2, 2002.

(35) Bard, A. J.; Faulkner, L. R. *Electrochemical Methods: Fundamentals and*

Applications, 2nd.; John Wiley & Sons, Inc.: Hoboken, NJ, USA, 2001.

(36) Marioli, J. M.; Kuwana, T. Electrochemical Characterization of Carbohydrate Oxidation at Copper Electrodes. *Electrochim. Acta* **1992**, *37* (7), 1187–1197. https://doi.org/10.1016/0013-4686(92)85055-P.

(37) Kok, W. T.; Brinkman, U. A. T.; Frei, R. W. Amperometric Detection of Amino Acids in High-Performance Liquid Chromatography with a Copper Electrode. *J. Chromatogr. A* **1983**, *256* (C), 17–26. https://doi.org/10.1016/S0021-9673(01)88208-X.

(38) Hancock, W. S.; Bishop, C. A.; Hearn, M. T. W. The Analysis of Nanogram Levels of Free Amino Acids by Reverse-Phase High-Pressure Liquid Chromatography. *Anal. Biochem.* **1979**, *92* (1), 170–173. https://doi.org/10.1016/0003-2697(79)90640-7.

(39) Loscombe, C. R.; Cox, G. B.; Dalziel, J. A. W. Application of a Copper Electrode as a Detector for High-Peformance Liquid Chromatography. *J. Chromatogr. A* **1978**, *166* (2), 403–410. https://doi.org/10.1016/S0021-9673(00)95623-1.

(40) Alexander, P. W.; Haddad, P. R.; Low, G. K. C.; Maitra, C. Application of a Copper Tubular Electrode as a Potentiometric Detector in the Determination of Amino Acids by High-Performance Liquid Chromatography. *J. Chromatogr. A* **1981**, *209* (1), 29–39. https://doi.org/10.1016/S0021-9673(00)80420-3.

(41) Tsuji, K.; Morozowich, W. GLC and HPLC Determination of Therapeutic Agents. *Ther. Drug Monit.* **1978**, *1* (4), 563. https://doi.org/10.1097/00007691-197910000-00013.

(42) Lee, H. M.; Forde, M. D.; Lee, M. C.; Bucher, D. J. Fluorometric Microbore Amino

Acid Analyzer: The Construction of an Inexpensive, Highly Sensitive Instrument Using o-Phthalaldehyde as a Detection Agent. *Anal. Biochem.* **1979**, *96* (2), 298–307. https://doi.org/10.1016/0003-2697(79)90585-2.

(43) Yui, Y.; Kawai, C. Comparison of the Sensitivity of Various Post-Column Methods for Catecholamine Analysis by High-Performance Liquid Chromatography. *J. Chromatogr. A* **1981**, *206* (3), 586–588. https://doi.org/10.1016/S0021-9673(00)88929-3.

(44) Ueda, T.; Mitchell, R.; Kitamura, F.; Nakamoto, A. Constant-Potential Amperometric Detection of Carbohydrates at Metal Electrodes in High-Performance Anion-Exchange Chromatography. *J. Chromatogr. A* **1992**, *592* (1–2), 229–237. https://doi.org/10.1016/0021-9673(92)85089-C.

(45) Ye, J.; Baldwin, R. P. Determination of Carbohydrates, Sugar Acids and Alditols by Capillary Electrophoresis and Electrochemical Detection at a Copper Electrode. *J. Chromatogr. A* **1994**, *687* (1), 141–148. https://doi.org/10.1016/0021-9673(94)00783-7.

(46) Kano, K.; Takagi, K.; Inoue, K.; Ikeda, T.; Ueda, T. Copper Electrodes for Stable Subpicomole Detection of Carbohydrates in High-Performance Liquid Chromatography. *J. Chromatogr. A* **1996**, *721* (1), 53–57. https://doi.org/10.1016/0021-9673(95)00757-1.

(47) Drew P. Manica, †; Yutaro Mitsumori, ‡ and; Andrew G. Ewing*, †. Characterization of Electrode Fouling and Surface Regeneration for a Platinum Electrode on an Electrophoresis Microchip. *Anal. Chem.* **2003**, *75* (17), 4572–4577. https://doi.org/10.1021/AC034235F.

(48) Bandwar, R. P.; Srinivasa Raghavan, M. S.; Rao, C. P. Transition Metal-Saccharide Chemistry: D-Glucose Complexes of Mn(II), Co(II), Ni(II), Cu(II) and Zn(II). *Biometals* **1995**, *8* (1), 19–24. https://doi.org/10.1007/BF00156153.

(49) Fleischmann, M.; Korinek, K.; Pletcher, D. The Kinetics and Mechanism of the Oxidation of Amines and Alcohols at Oxide-Covered Nickel, Silver, Copper, and Cobalt Electrodes. *J. Chem. Soc. Perkin Trans. 2* **1972**, No. 10, 1396–1403. https://doi.org/10.1039/p29720001396.

(50) Navarro, M.; May, P. M.; Hefter, G.; Königsberger, E. Solubility of CuO(s) in Highly Alkaline Solutions. *Hydrometallurgy* **2014**, *147–148*, 68–72. https://doi.org/10.1016/j.hydromet.2014.04.018.

(51) Striegler, S.; Tewes, E. Investigation of Sugar-Binding Sites in Ternary Ligand−Copper(II)−Carbohydrate Complexes. *Eur. J. Inorg. Chem.* **2002**, *2002* (2), 487–495. https://doi.org/10.1002/1099-0682(20022)2002:2<487::AID-EJIC487>3.0.CO;2-D.

(52) Cerchiaro, G.; Sant'Ana, A. C.; Arruda Temperini, M. L.; Da Costa Ferreira, A. M. Investigations of Different Carbohydrate Anomers in Copper(II) Complexes with D-Glucose, D-Fructose, and D-Galactose by Raman and EPR Spectroscopy. *Carbohydr. Res.* **2005**, *340* (15), 2352–2359. https://doi.org/10.1016/j.carres.2005.08.002.

(53) Alekseev, Y. E.; Garnovskii, A. D.; Zhdanov, Y. A. Complexes of Natural Carbohydrates with Metal Cations. *Usp. Khim.* **1998**, *67* (8), 738–744. https://doi.org/10.1070/rc1998v067n08abeh000343.

(54) *Ion Chromatography, Volume 46 - 1st Edition*; Haddad, P. R., Jackson, P. E.,

Eds.; Elsevier, 1990; Vol. 46.

(55) Mo, Y. Investigations in Capillary Liquid Chromatography. **1997**, 50–52.

(56) Shelor, C. P.; Liao, H.; Kadjo, A. F.; Dasgupta, P. K. Enigmatic Ion-Exchange Behavior of Myo-Inositol Phosphates. *Anal. Chem.* **2015**, *87* (9), 4851–4855. https://doi.org/10.1021/ACS.ANALCHEM.5B00351.